

# Combined study of the isospin-violating decay $D_s^* \rightarrow D_s \pi^0$ and radiative decay $D_s^* \rightarrow D_s \gamma$ with intermediate meson loops

Jun Wang<sup>1,2\*</sup> and Qiang Zhao<sup>1,2,3†</sup>

<sup>1</sup> *Institute of High Energy Physics, Chinese Academy of Sciences, Beijing 100049, China*

<sup>2</sup> *University of Chinese Academy of Sciences, Beijing 100049, China*

<sup>3</sup> *Center for High Energy Physics, Henan Academy of Sciences, Zhengzhou 450046, China*

We carry out a combined study of the isospin-violating decay  $D_s^* \rightarrow D_s \pi^0$  and radiative decay  $D_s^* \rightarrow D_s \gamma$  in an effective Lagrangian approach by taking into account the corrections from the one-loop transitions. By distinguishing the transition mechanisms of the long-distance interactions through the intermediate meson loops from the short-distance interactions through the  $\eta - \pi^0$  mixing at the tree level the isospin-violating decay  $D_s^* \rightarrow D_s \pi^0$  can be well constrained. In our approach the higher order corrections to the isospin-violating effects can involve the intermediate  $D^{(*)}$  and  $K^{(*)}$  scatterings. We find that the contributions from the destructive interference of intermediate meson loops via  $D^{(*)0}(c\bar{u})K^{(*)+}(u\bar{s})$  and  $D^{(*)+}(c\bar{d})K^{(*)0}(d\bar{s})$  rescatterings are significant. Within the commonly accepted ultra-violet (UV) cutoff range we obtain the partial decay width  $\Gamma[D_s^* \rightarrow D_s \pi^0] = 9.92_{-0.66}^{+0.76}$  eV. This approach allows us to describe the  $D_s^*$  radiative decay in the same framework via the vector meson dominance (VMD) model. We demonstrate that both the tree-level and one-loop transitions can be self-consistently determined if we adopt the experimental data for the branching ratio fraction of  $D_s^* \rightarrow D_s \pi^0$  to  $D_s^* \rightarrow D_s \gamma$ . It then leads to a reliable estimate of the total decay width of  $D_s^*$ , i.e.  $\Gamma_{\text{total}}(D_s^{*+}) = 170_{-12}^{+13}$  eV.

## I. INTRODUCTION

The study of isospin symmetry and its violations in hadronic decays provides critical insights into the dynamics of strong interactions in the non-perturbative regime. While isospin symmetry is approximately conserved in strong processes, its breaking, often arising from mass differences between up and down quarks and/or electromagnetic effects, offers a unique window into subtle aspects of hadron structure and decay mechanisms. Among such processes, the decay  $D_s^* \rightarrow D_s \pi^0$ , which violates isospin symmetry, presents a compelling case for the detailed underlying dynamics. It is interesting to note that although the  $D_s^*$  has been observed in experiment for a long time, its quantum number as the ground state of the charmed-strange vector meson was just measured very recently [1]. But its total width is still not determined.

The strong and radiative decays of  $D_s^*$  has attracted a lot of attention in the literature. Due to the limited phase space and isospin violation, the branching ratio of  $D_s^* \rightarrow D_s \pi^0$  is much smaller than that of  $D_s^* \rightarrow D_s \gamma$ . While the radiative decay  $D_s^* \rightarrow D_s \gamma$  via an  $M1$  transition has a relatively well defined picture in the constituent quark model and there have been a lot of studies of the radiative transition [2–13], the isospin-violating decay of  $D_s^* \rightarrow D_s \pi^0$  has not yet been broadly investigated. Several recent works have been dedicated to this issue based on the  $\eta - \pi^0$  mixing [13–16]. In Ref. [17] a heavy meson chiral perturbation theory calculation was presented with the  $\mathcal{O}(p^3)$  loop corrections, and it was found that the  $\mathcal{O}(p^3)$  corrections may actually be significant.

On top of the  $\eta - \pi^0$  mixing scenario, corrections from higher-order mechanisms are the focus of attention which is correlated with the total width question about  $D_s^*$ . In the framework of the heavy meson chiral perturbation theory [17] it is shown that the next-to-leading-order loop diagrams of  $\mathcal{O}(p^3)$  are associated with the counter term tree diagrams of the same order, where four undetermined low energy constants (LECs) are involved. Delicate considerations of estimating the  $\mathcal{O}(p^3)$  tree diagram contributions are discussed in Ref. [17] and the corrections can amount to about 30% of the leading  $\eta \pi^0$  mixing effects. While more constraints of the LECs should be sought, alternative approaches should also be explored in order to elucidate the isospin breaking mechanism.

In this work we propose an effective Lagrangian approach for calculating the higher-order corrections of the isospin-violating decay  $D_s^* \rightarrow D_s \pi^0$ . In addition to the leading tree-level amplitude from the  $\eta - \pi^0$  mixing, we construct the higher-order corrections from the intermediate charmed meson  $D^{(*)}$  and strange meson  $K^{(*)}$  rescatterings. At the one-loop level the isospin-breaking can be categorized by two groups. One is the direct production of  $\pi^0$  via the destructive interferences between the two loop amplitudes, namely between the  $D^{(*)0}(c\bar{u})K^{(*)+}(u\bar{s})$  and  $D^{(*)+}(c\bar{d})K^{(*)0}(d\bar{s})$ . The other one is via the one-loop production of  $\eta$  and then via the mixing of  $\eta \pi^0$ . In the latter case there are two

\* junwang@ihep.ac.cn

† zhaoq@ihep.ac.cn

corresponding loops involving the  $u\bar{u}$  and  $d\bar{d}$  productions, respectively, and they have a constructive phase first to produce  $\eta$  and then couple to  $\pi^0$  via the  $\eta - \pi^0$  mixing. It should be noted that these two groups are not double-counting.

It should also be noted that although the one-loop intermediate meson rescattering amplitudes do not simply count corrections of  $\mathcal{O}(p^3)$ , the leading one-loop amplitude provides corrections to the tree-level mixing term at  $\mathcal{O}(m_\pi/m_{ex})$ , where  $m_{ex}$  is the exchanged meson mass between these two intermediate mesons, i.e.  $D^{(*)}$  and  $K^{(*)}$ . We include all the ground-state vector and pseudoscalar meson rescatterings in the one-loop amplitude of which the vertex couplings can be well determined by either experimental measurements or heavy quark symmetry and chiral symmetry relations [18–20]. These amplitudes are unified by an overall cut-off parameter which is introduced with a form factor to regularize the loop integrals. In this sense, the model uncertainties will be contained in the cutoff parameter, and the stability of the one-loop contributions can serve as a criterion for the model-dependent aspect of this approach. This method has been broadly applied to the studies of various isospin symmetry breaking processes [21–24] and the helicity selection rule violation processes [25–27] in the literature.

In the same framework we can then extend the study to the  $D_s^*$  radiative decay via the vector meson dominance (VMD) model. The leading tree-level transition of  $D_s^* \rightarrow D_s\gamma$  will go through the intermediate flavor neutral vector meson production followed by the vector meson conversion into the final-state photon. This can be categorized as the short-distance part of the radiative transition. Similar to the isospin-violating decay process, we can define the long-distance transition by the one-loop intermediate meson rescatterings where the vector meson will then convert into the final-state photon. Thus, these two dominant decay channels, i.e.  $D_s^* \rightarrow D_s\gamma$  and  $D_s^* \rightarrow D_s\pi^0$  can be combined together with the same set of parameters except for one different coupling parameter  $g_{J/\psi D\bar{D}}$  introduced in  $D_s^* \rightarrow D_s\gamma$ . Their relative strength, i.e. the relative branching ratio fraction between  $D_s^* \rightarrow D_s\gamma$  and  $D_s^* \rightarrow D_s\pi^0$ , will provide a strong constraint on  $g_{J/\psi D\bar{D}}$  in  $D_s^* \rightarrow D_s\gamma$ . Since this parameter can be determined by other independent processes, our calculation can examine the self-consistency of the formalism by comparing the constrained value for  $g_{J/\psi D\bar{D}}$  with its commonly adopted values. Such a consistent constraint then allows us to extract the total width for  $D_s^*$ .

As follows, we first introduce our formalism in Sec. II. The numerical results and discussions will be presented in Sec. III. A brief summary and conclusion will be given in Sec. IV.

## II. FORMALISM

Our approach for the isospin-violating decay of  $D_s^{*+} \rightarrow D_s^+\pi^0$  contains two main ingredients. The first one is the tree-level transition via the  $\eta - \pi^0$  mixing. The second one is the loop transition via the intermediate  $D^{(*)}$  and  $K^{(*)}$  rescatterings. The electromagnetic transition contributions to the isospin-violating decay in  $D_s^{*+} \rightarrow D_s^+\pi^0$  is believed to be negligibly small [14, 17].

For  $D_s^* \rightarrow D_s\gamma$ , we calculate the leading  $M_1$  transition in the VMD model where the  $D_s^*$  first couples to  $D_s\phi$  and  $D_s J/\psi$ , and then the vector mesons will convert into photon via the VMD mechanism. We also consider the one-loop correction in the same framework. The the intermediate  $D^{(*)}$  and  $K^{(*)}$  rescatterings will produce  $D_s$  and the flavor neutral vector mesons and the latters will then convert into photon via the VMD mechanism.

In this unified framework the effective Lagrangians are constructed by taking into account both the heavy quark symmetry and chiral symmetry [18–20]. The photon-vector-meson couplings can be determined by the leptonic decays of the vector mesons in  $V \rightarrow e^+e^-$  with the help of the experimental measurements [28].

### A. Effective Lagrangians

To describe the strong couplings the following effective Lagrangians [20, 29, 30] are adopted :

$$\begin{aligned} \mathcal{L} = & -ig_{\mathcal{D}^*\mathcal{D}\mathcal{P}}(\mathcal{D}^i\partial^\mu\mathcal{P}_{ij}\mathcal{D}_\mu^{*j\dagger} - \mathcal{D}_\mu^{*i}\partial^\mu\mathcal{P}_{ij}\mathcal{D}^{j\dagger}) + \frac{1}{2}g_{\mathcal{D}^*\mathcal{D}^*\mathcal{P}}\varepsilon_{\mu\nu\alpha\beta}\mathcal{D}_i^{*\mu}\partial^\nu\mathcal{P}^{ij}\overleftrightarrow{\partial}^\alpha\mathcal{D}_j^{*\beta\dagger} \\ & -ig_{\mathcal{D}\mathcal{D}\mathcal{V}}\mathcal{D}_i^\dagger\overleftrightarrow{\partial}_\mu\mathcal{D}^j(\mathcal{V}^\mu)_j^i - 2f_{\mathcal{D}^*\mathcal{D}\mathcal{V}}\varepsilon_{\mu\nu\alpha\beta}(\partial^\mu\mathcal{V}^\nu)_j^i(\mathcal{D}_i^\dagger\overleftrightarrow{\partial}^\alpha\mathcal{D}^{*\beta j} - \mathcal{D}_i^{*\beta\dagger}\overleftrightarrow{\partial}^\alpha\mathcal{D}^j) \\ & +ig_{\mathcal{D}^*\mathcal{D}^*\mathcal{V}}\mathcal{D}_i^{*\nu\dagger}\overleftrightarrow{\partial}_\mu\mathcal{D}_\nu^{*j}(\mathcal{V}^\mu)_j^i + 4if_{\mathcal{D}^*\mathcal{D}^*\mathcal{V}}\mathcal{D}_{i\mu}^{*\dagger}(\partial^\mu\mathcal{V}^\nu - \partial^\nu\mathcal{V}^\mu)_j^i\mathcal{D}_\nu^{*j}, \end{aligned} \quad (1)$$

where  $\mathcal{D}$  and  $\mathcal{D}^*$  represent the pseudoscalar and vector charm meson fields, respectively, i.e.

$$\mathcal{D} = (D^0, D^+, D_s^+), \quad \mathcal{D}^* = (D^{*0}, D^{*+}, D_s^{*+}), \quad (2)$$

$\mathcal{P}$  and  $\mathcal{V}$  are  $3 \times 3$  matrices representing the pseudoscalar nonet and vector nonet meson fields [31]

$$\mathcal{P} = \begin{pmatrix} \frac{\sin \alpha_P \eta' + \cos \alpha_P \eta + \pi^0}{\sqrt{2}} & \pi^+ & K^+ \\ \pi^- & \frac{\sin \alpha_P \eta' + \cos \alpha_P \eta - \pi^0}{\sqrt{2}} & K^0 \\ K^- & \bar{K}^0 & \cos \alpha_P \eta' - \sin \alpha_P \eta \end{pmatrix} \quad \mathcal{V} = \begin{pmatrix} \frac{\rho^0 + \omega}{\sqrt{2}} & \rho^+ & K^{*+} \\ \rho^- & \frac{\omega - \rho^0}{\sqrt{2}} & K^{*0} \\ K^{*-} & \bar{K}^{*0} & \phi \end{pmatrix}. \quad (3)$$

Specifically, for the process  $D_s^{*+} \rightarrow D_s^+ \eta$ , the corresponding effective Lagrangian is

$$\mathcal{L}_{D_s^* D_s \eta} = i g_{\mathcal{D}^* \mathcal{D} \mathcal{P}} \sin \alpha_P D_s (D_s^*)_\mu \partial^\mu \eta. \quad (4)$$

where  $\alpha_P = 40.6^\circ$  is the  $\eta$ - $\eta'$  mixing angle in the SU(3) flavor basis, and the value is an average from the Particle Data Group [28]. For the  $\eta \rightarrow \pi^0$  process, we use the  $\eta - \pi^0$  mixing angle  $\theta_{\eta\pi^0}$  which is given by the leading order chiral expansion [32]

$$\tan(2\theta_{\eta\pi^0}) = \frac{\sqrt{3} m_d - m_u}{2 m_s - \hat{m}}. \quad (5)$$

where  $\hat{m} = (m_u + m_d)/2$ . The values of  $m_u$ ,  $m_d$ , and  $m_s$  are taken from the Particle Data Group [28]. Since  $\theta_{\eta\pi^0}$  is very small, we take

$$\theta_{\eta\pi^0} \simeq \frac{\sqrt{3} m_d - m_u}{4 m_s - \hat{m}}, \quad (6)$$

as broadly adopted in the literature.

For the light hadron vertices, we adopt the following effective Lagrangian:

$$\begin{aligned} \mathcal{L}_{VPP} &= i g_{VPP} \text{Tr}[(\mathcal{P} \partial_\mu \mathcal{P} - \partial_\mu \mathcal{P} \mathcal{P}) \mathcal{V}^\mu], \\ \mathcal{L}_{VVP} &= g_{VVP} \varepsilon_{\alpha\beta\mu\nu} \text{Tr}[\partial^\alpha \mathcal{V}^\mu \partial^\beta \mathcal{V}^\nu \mathcal{P}], \\ \mathcal{L}_{VVV} &= i g_{VVV} \text{Tr}[(\partial_\mu V_\nu - \partial_\nu V_\mu) V^\mu V^\nu]. \end{aligned} \quad (7)$$

For the coupling constants of  $D$  mesons and light mesons, we adopt the following results [23, 27, 29, 30, 33]

$$\begin{aligned} g_{D^* D^* \pi} &= \frac{g_{D^* D \pi}}{\sqrt{m_D m_{D^*}}} = \frac{2g}{f_\pi}, \quad g_{DDV} = g_{D^* D^* V} = \frac{\beta g_V}{\sqrt{2}}, \quad f_{D^* DV} = \frac{f_{D^* D^* V}}{m_{D^*}} = \frac{\lambda g_V}{\sqrt{2}}, \quad g_{D^* D_s K} = \sqrt{\frac{m_{D_s}}{m_D}} g_{D^* D \pi}, \\ g_{D_s^* DK} &= \sqrt{\frac{m_{D_s^*}}{m_{D^*}}} g_{D^* D \pi}, \quad g_V = \frac{m_\rho}{f_\pi}, \quad g_{D^* D^* K} = \frac{g_{D^* DK}}{\sqrt{m_D m_{D^*}}} = \frac{2g}{f_K}, \quad g_{D_s DV} = \sqrt{\frac{m_{D_s}}{m_D}} g_{DDV}, \\ g_{D^* D_s^* K^*} &= \sqrt{\frac{m_{D_s^*}}{m_{D^*}}} g_{D^* D^* V}, \quad f_{D^* D_s^* K^*} = \sqrt{\frac{m_{D_s^*}}{m_{D^*}}} f_{D^* D^* V}, \quad \frac{g_{D_s^* D_s \eta}}{\sqrt{m_{D_s^*} m_{D_s}}} = \frac{g_{D^* D \pi} \sin \alpha_P}{\sqrt{m_{D^*} m_D}}. \end{aligned} \quad (8)$$

where  $g = 0.59$ ,  $\beta = 0.9$ ,  $f_\pi = 132$  MeV,  $f_K = 155$  MeV and  $\lambda = 0.56$  GeV<sup>-1</sup> are adopted [23, 27, 29, 30, 34].

The relative strengths and phases of the coupling constants for vector and scalar mesons can be determined by SU(3) flavor symmetry relations, and expressed by overall coupling constants  $g_{VVP}$  and  $g_{VPP}$  [31],

$$\begin{aligned} g_{K^{*+} K^{*-} \pi^0} &= -g_{K^{*0} \bar{K}^{*0} \pi^0} = \frac{1}{\sqrt{2}} g_{VVP}, \\ g_{K^{*0} \bar{K}^0 \pi^0} &= -g_{K^{*0} \pi^0 \bar{K}^0} = g_{\bar{K}^{*0} \pi^0 K^0} = -g_{\bar{K}^{*0} K^0 \pi^0} = \frac{1}{\sqrt{2}} g_{VPP}, \\ g_{K^{*+} \pi^0 K^-} &= -g_{K^{*+} K^- \pi^0} = g_{K^{*-} K^+ \pi^0} = -g_{K^{*-} \pi^0 K^+} = \frac{1}{\sqrt{2}} g_{VPP}. \end{aligned} \quad (9)$$

## B. Tree and loop transition amplitudes of $D_s^{*+} \rightarrow D_s^+ \pi^0$

Based on the effective Lagrangians in the previous section, we can derive the tree and loop amplitudes in order as follows. For the tree-level amplitude corresponding to Fig. 1, we have

$$i\mathcal{M}_{\text{tree}} = i g_{D_s^* D_s \eta} \varepsilon_{D_s^*} \cdot p_3 \theta_{\eta\pi^0} = i g_{\text{tree}} \varepsilon_{D_s^*} \cdot (p_2 - p_3), \quad (10)$$

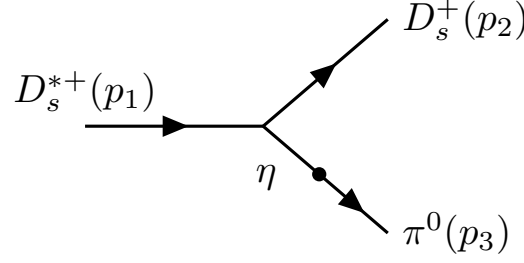


FIG. 1: Schematic diagrams of the decay  $D_s^{*+} \rightarrow D_s^+ \pi^0$  via the  $\eta - \pi^0$  mixing at tree level.

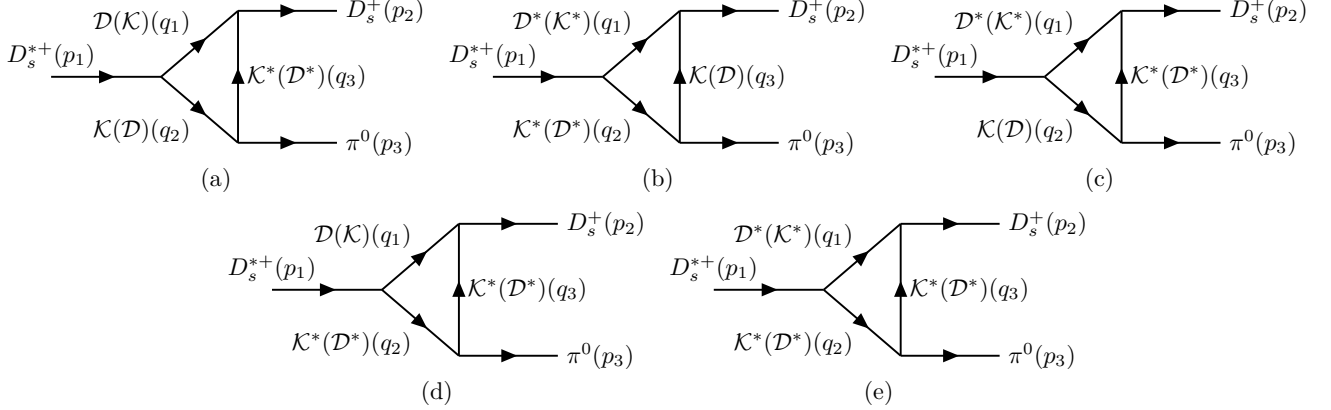


FIG. 2: Schematic diagrams of the decay  $D_s^{*+} \rightarrow D_s^+ \pi^0$  via intermediate meson loops, where  $\mathcal{D} = (D^+, D^0)$  and  $\mathcal{K} = (K^+, K^0)$ .

where  $g_{\text{tree}} \equiv g_{D_s^* D_s \eta} \theta_{\eta \pi^0} / 2$  in our convention.

For the loop-level amplitudes without the  $\eta - \pi^0$  mixing corresponding to Fig. 2, we denote the amplitude as  $i\mathcal{M}(P_1, P_2, P_3)$ , where  $P_i$  represents the intermediate meson with momentum  $q_i$ ,  $\varepsilon^s$  is the polarization vector of the initial state  $D_s^*$ , and  $\varepsilon^i$  is the polarization vector of the intermediate meson with momentum  $q_i$ . So the amplitudes corresponding to Fig. 2 can be expressed as

$$i\mathcal{M}_a(\mathcal{D}, \mathcal{K}, \mathcal{K}^*) = \int \frac{d^4 q_3}{(2\pi)^4} \frac{g_{\mathcal{D}^* \mathcal{D} \mathcal{K} q_2} \cdot \varepsilon^s g_{\mathcal{D}_s \mathcal{D} \mathcal{K}^*} (q_1 + p_2)_\alpha \left( g^{\alpha\beta} - \frac{q_3^\alpha q_3^\beta}{m_3^2} \right) g_{\mathcal{K}^* \mathcal{K} \pi} (p_3 + q_2)_\beta}{(q_1^2 - m_1^2)(q_2^2 - m_2^2)(q_3^2 - m_3^2)} \mathcal{F}(q_i^2), \quad (11)$$

$$i\mathcal{M}_a(\mathcal{K}, \mathcal{D}, \mathcal{D}^*) = \int \frac{d^4 q_3}{(2\pi)^4} \frac{g_{\mathcal{D}^* \mathcal{D} \mathcal{K} q_2} g_{\mathcal{D}^* \mathcal{D}_s \mathcal{K} q_1} \cdot \varepsilon^s q_1^\mu \left( g_{\mu\nu} - \frac{q_3^\mu q_3^\nu}{m_3^2} \right) p_3^\nu}{(q_1^2 - m_1^2)(q_2^2 - m_2^2)(q_3^2 - m_3^2)} \mathcal{F}(q_i^2), \quad (12)$$

$$i\mathcal{M}_b(\mathcal{D}^*, \mathcal{K}^*, \mathcal{K}) = \int \frac{d^4 q_3}{(2\pi)^4} \frac{(g_{\mathcal{D}^* \mathcal{D}^* \mathcal{K}^*} (p_1^\mu + q_1^\mu) g^{\alpha\beta} - 4f_{\mathcal{D}^* \mathcal{D}^* \mathcal{K}^*} (q_2^\beta g^{\alpha\mu} - q_2^\alpha g^{\beta\mu})) \varepsilon_\alpha^s g_{\mathcal{D}^* \mathcal{D}_s \mathcal{K} q_3}^\nu}{(q_1^2 - m_1^2)(q_2^2 - m_2^2)(q_3^2 - m_3^2)} \\ \times g_{\mathcal{K}^* \mathcal{K} \pi} (p_3^\lambda - q_3^\lambda) \left( g_{\beta\nu} - \frac{q_{1\beta} q_{1\nu}}{m_1^2} \right) \left( g_{\mu\lambda} - \frac{q_{2\mu} q_{2\lambda}}{m_2^2} \right) \mathcal{F}(q_i^2), \quad (13)$$

$$i\mathcal{M}_b(\mathcal{K}^*, \mathcal{D}^*, \mathcal{D}) = - \int \frac{d^4 q_3}{(2\pi)^4} \frac{(g_{\mathcal{D}^* \mathcal{D}^* \mathcal{K}^*} (p_1^\mu + q_2^\mu) g^{\alpha\beta} - 4f_{\mathcal{D}^* \mathcal{D}^* \mathcal{K}^*} (q_1^\beta g^{\alpha\mu} - q_1^\alpha g^{\beta\mu})) \varepsilon_\alpha^s g_{\mathcal{D}^* \mathcal{D}_s \mathcal{K} q_3}^\lambda}{(q_1^2 - m_1^2)(q_2^2 - m_2^2)(q_3^2 - m_3^2)} \\ \times g_{\mathcal{D}_s \mathcal{D} \mathcal{K}^*} (p_2 + q_3)^\nu \left( g_{\beta\nu} - \frac{q_{1\beta} q_{1\nu}}{m_1^2} \right) \left( g_{\mu\lambda} - \frac{q_{2\mu} q_{2\lambda}}{m_2^2} \right) \mathcal{F}(q_i^2), \quad (14)$$

$$i\mathcal{M}_c(\mathcal{D}^*, \mathcal{K}, \mathcal{K}^*) = - \int \frac{d^4 q_3}{(2\pi)^4} \frac{4g_{\mathcal{D}^* \mathcal{D}^* \mathcal{K}^*} \varepsilon_{\mu\nu\alpha\beta} p_1^\nu \varepsilon^{\sigma\mu} q_1^\alpha f_{\mathcal{D}^* \mathcal{D}_s \mathcal{K}^*} \varepsilon_{\kappa\sigma\zeta\rho} q_3^\kappa p_2^\zeta}{(q_1^2 - m_1^2)(q_2^2 - m_2^2)(q_3^2 - m_3^2)} \\ \times g_{\mathcal{K}^* \mathcal{K} \pi} (p_{3\lambda} + q_{2\lambda}) \left( g^{\beta\rho} - \frac{q_1^\beta q_1^\rho}{m_1^2} \right) \left( g^{\sigma\lambda} - \frac{q_3^\sigma q_3^\lambda}{m_3^2} \right) \mathcal{F}(q_i^2), \quad (15)$$

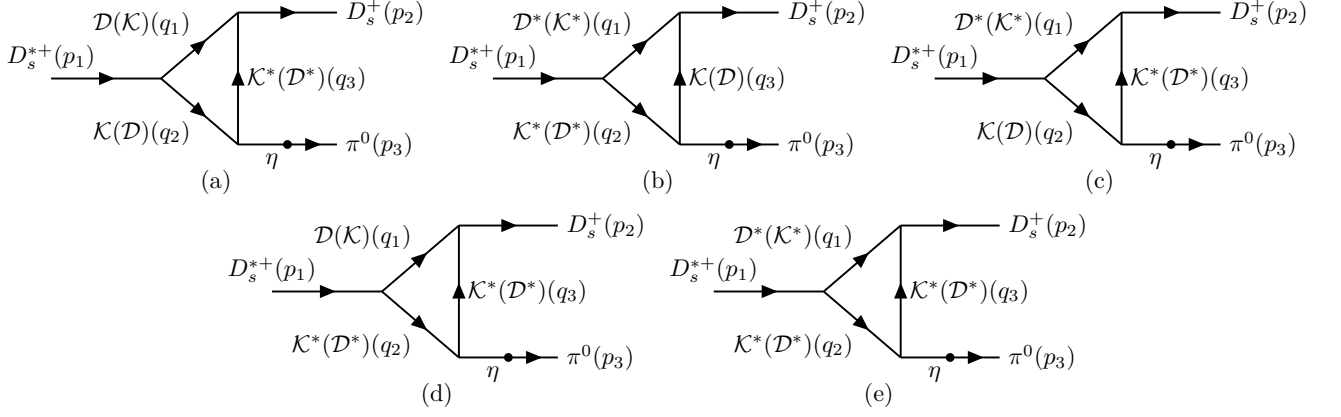


FIG. 3: Schematic diagrams of the decay  $D_s^{*+} \rightarrow D_s^+ \pi^0$  via intermediate meson loops and  $\eta - \pi$  mixing, where  $\mathcal{D} = (D^+, D^0)$  and  $\mathcal{K} = (K^+, K^0)$ .

$$i\mathcal{M}_c(\mathcal{K}^*, \mathcal{D}, \mathcal{D}^*) = - \int \frac{d^4 q_3}{(2\pi)^4} \frac{16 f_{\mathcal{D}_s^*} \mathcal{D} \mathcal{K}^* \varepsilon_{\alpha\beta\tau\mu} q_1^\alpha q_2^\tau \varepsilon^{s\mu} f_{\mathcal{D}^*} \mathcal{D}_s \mathcal{K}^* \varepsilon_{\kappa\rho\zeta\sigma} q_1^\kappa p_2^\zeta}{(q_1^2 - m_1^2)(q_2^2 - m_2^2)(q_3^2 - m_3^2)} \times g_{\mathcal{D}^* \mathcal{D} \pi} p_{3\lambda} \left( g^{\beta\rho} - \frac{q_1^\beta q_1^\rho}{m_1^2} \right) \left( g^{\sigma\lambda} - \frac{q_3^\sigma q_3^\lambda}{m_3^2} \right) \mathcal{F}(q_i^2), \quad (16)$$

$$i\mathcal{M}_d(\mathcal{D}, \mathcal{K}^*, \mathcal{K}^*) = \int \frac{d^4 q_3}{(2\pi)^4} \frac{4 f_{\mathcal{D}_s^*} \mathcal{D} \mathcal{K}^* \varepsilon_{\alpha\beta\tau\mu} q_2^\alpha q_1^\tau \varepsilon^{s\mu} g_{\mathcal{D} \mathcal{D}_s \mathcal{K}^*} (q_1 + p_2)_\sigma}{(q_1^2 - m_1^2)(q_2^2 - m_2^2)(q_3^2 - m_3^2)} \times g_{\mathcal{K}^* \mathcal{K}^* \pi} \varepsilon_{\kappa\zeta\rho\lambda} q_2^\kappa q_3^\zeta \left( g^{\beta\rho} - \frac{q_2^\beta q_2^\rho}{m_2^2} \right) \left( g^{\sigma\lambda} - \frac{q_3^\sigma q_3^\lambda}{m_3^2} \right) \mathcal{F}(q_i^2), \quad (17)$$

$$i\mathcal{M}_d(\mathcal{K}, \mathcal{D}^*, \mathcal{D}^*) = - \int \frac{d^4 q_3}{(2\pi)^4} \frac{g_{\mathcal{D}_s^* \mathcal{D}^* \mathcal{K}} \varepsilon_{\mu\nu\alpha\beta} p_1^\nu \varepsilon^{s\mu} q_2^\alpha g_{\mathcal{D}^* \mathcal{D}_s \mathcal{K}} q_1^\sigma}{(q_1^2 - m_1^2)(q_2^2 - m_2^2)(q_3^2 - m_3^2)} \times g_{\mathcal{D}^* \mathcal{D}^* \pi} \varepsilon_{\rho\zeta\kappa\lambda} p_3^\zeta q_3^\kappa \left( g^{\beta\rho} - \frac{q_2^\beta q_2^\rho}{m_2^2} \right) \left( g^{\sigma\lambda} - \frac{q_3^\sigma q_3^\lambda}{m_3^2} \right) \mathcal{F}(q_i^2), \quad (18)$$

$$i\mathcal{M}_e(\mathcal{D}^*, \mathcal{K}^*, \mathcal{K}^*) = \int \frac{d^4 q_3}{(2\pi)^4} \frac{4(g_{\mathcal{D}_s^* \mathcal{D}^* \mathcal{K}^*} (p_1 + q_1)_\mu g_{\alpha\beta} - 4f_{\mathcal{D}_s^*} \mathcal{D}^* \mathcal{K}^* (q_2)_\beta g_{\alpha\mu} - q_2)_\alpha g_{\beta\mu}) \varepsilon^{s\alpha}}{(q_1^2 - m_1^2)(q_2^2 - m_2^2)(q_3^2 - m_3^2)} \times f_{\mathcal{D}^* \mathcal{D}_s \mathcal{K}^*} \varepsilon_{\kappa\sigma\zeta\rho} q_3^\kappa p_2^\zeta g_{\mathcal{K}^* \mathcal{K}^* \pi} \varepsilon_{\tau\delta\nu\lambda} q_2^\tau q_3^\delta \times \left( g^{\beta\rho} - \frac{q_1^\beta q_1^\rho}{m_1^2} \right) \left( g^{\mu\nu} - \frac{q_2^\mu q_2^\nu}{m_2^2} \right) \left( g^{\sigma\lambda} - \frac{q_3^\sigma q_3^\lambda}{m_3^2} \right) \mathcal{F}(q_i^2), \quad (19)$$

$$i\mathcal{M}_e(\mathcal{K}^*, \mathcal{D}^*, \mathcal{D}^*) = \int \frac{d^4 q_3}{(2\pi)^4} \frac{4(g_{\mathcal{D}_s^* \mathcal{D}^* \mathcal{K}^*} (p_1 + q_2)_\beta g_{\alpha\mu} - 4f_{\mathcal{D}_s^*} \mathcal{D}^* \mathcal{K}^* (q_1)_\mu g_{\alpha\beta} - q_1)_\alpha g_{\beta\mu}) \varepsilon^{s\alpha}}{(q_1^2 - m_1^2)(q_2^2 - m_2^2)(q_3^2 - m_3^2)} \times f_{\mathcal{D}^* \mathcal{D}_s \mathcal{K}^*} \varepsilon_{\kappa\rho\zeta\sigma} q_1^\kappa p_2^\zeta g_{\mathcal{D}^* \mathcal{D}^* \pi} \varepsilon_{\nu\tau\delta\lambda} p_3^\tau q_3^\delta \times \left( g^{\beta\rho} - \frac{q_1^\beta q_1^\rho}{m_1^2} \right) \left( g^{\mu\nu} - \frac{q_2^\mu q_2^\nu}{m_2^2} \right) \left( g^{\sigma\lambda} - \frac{q_3^\sigma q_3^\lambda}{m_3^2} \right) \mathcal{F}(q_i^2). \quad (20)$$

In the above equations  $\mathcal{F}(q_i^2)$  is a form factor adopted for cutting off the ultraviolet divergence in the loop integrals, and has the following form

$$\mathcal{F}(p_i^2) = \prod_i \left( \frac{\Lambda_i^2 - m_i^2}{\Lambda_i^2 - p_i^2} \right), \quad (21)$$

where  $\Lambda_i \equiv m_i + \alpha \Lambda_{\text{QCD}}$  with the  $m_i$  the mass of the  $i$ th internal particle, and the QCD energy scale  $\Lambda_{\text{QCD}} = 220 \text{ MeV}$  with  $\alpha = 1 \sim 2$  as the cutoff parameter [24, 35].

For the loop diagrams involving the  $\eta - \pi^0$  mixing corresponding to Fig. 3, the difference from the loop diagrams of Fig. 2 lies in the coupling constants related to  $\eta$  and  $\pi$ . Namely, for those two isospin-related channels, their amplitudes

will have a constructive phase in the  $D_s^* \rightarrow D_s \eta$  transition, but will have a destructive phase in  $D_s^* \rightarrow D_s \pi^0$ .

The  $\eta$  production amplitudes via the triangle loops will contribute to the  $D_s^* \rightarrow D_s \pi^0$  channel via the  $\eta - \pi^0$  mixing. We denote the amplitude as  $i\mathcal{M}(P_1, P_2, P_3, \eta)$  and for each process in Fig. 3 their expressions are given below:

$$i\mathcal{M}_a(\mathcal{D}, \mathcal{K}, \mathcal{K}^*, \eta) = i\mathcal{M}_a(\mathcal{D}, \mathcal{K}, \mathcal{K}^*) \cdot \frac{g\mathcal{K}\mathcal{K}^*\eta\theta_{\eta\pi^0}}{g\mathcal{K}\mathcal{K}^*\pi}, \quad i\mathcal{M}_a(\mathcal{K}, \mathcal{D}, \mathcal{D}^*, \eta) = i\mathcal{M}_a(\mathcal{K}, \mathcal{D}, \mathcal{D}^*) \cdot \frac{g\mathcal{D}^*\mathcal{D}\eta\theta_{\eta\pi^0}}{g\mathcal{D}^*\mathcal{D}\pi}, \quad (22)$$

$$i\mathcal{M}_b(\mathcal{D}^*, \mathcal{K}^*, \mathcal{K}, \eta) = i\mathcal{M}_b(\mathcal{D}^*, \mathcal{K}^*, \mathcal{K}) \cdot \frac{g\mathcal{K}\mathcal{K}^*\eta\theta_{\eta\pi^0}}{g\mathcal{K}\mathcal{K}^*\pi}, \quad i\mathcal{M}_b(\mathcal{K}^*, \mathcal{D}^*, \mathcal{D}, \eta) = i\mathcal{M}_b(\mathcal{K}^*, \mathcal{D}^*, \mathcal{D}) \cdot \frac{g\mathcal{D}^*\mathcal{D}\eta\theta_{\eta\pi^0}}{g\mathcal{D}^*\mathcal{D}\pi}, \quad (23)$$

$$i\mathcal{M}_c(\mathcal{D}^*, \mathcal{K}, \mathcal{K}^*, \eta) = i\mathcal{M}_c(\mathcal{D}^*, \mathcal{K}, \mathcal{K}^*) \cdot \frac{g\mathcal{K}\mathcal{K}^*\eta\theta_{\eta\pi^0}}{g\mathcal{K}\mathcal{K}^*\pi}, \quad i\mathcal{M}_c(\mathcal{K}^*, \mathcal{D}, \mathcal{D}^*, \eta) = i\mathcal{M}_c(\mathcal{K}^*, \mathcal{D}, \mathcal{D}^*) \cdot \frac{g\mathcal{D}^*\mathcal{D}\eta\theta_{\eta\pi^0}}{g\mathcal{D}^*\mathcal{D}\pi}, \quad (24)$$

$$i\mathcal{M}_d(\mathcal{D}, \mathcal{K}^*, \mathcal{K}^*, \eta) = i\mathcal{M}_d(\mathcal{D}, \mathcal{K}^*, \mathcal{K}^*) \cdot \frac{g\mathcal{K}^*\mathcal{K}^*\eta\theta_{\eta\pi^0}}{g\mathcal{K}^*\mathcal{K}^*\pi}, \quad i\mathcal{M}_d(\mathcal{K}, \mathcal{D}^*, \mathcal{D}^*, \eta) = i\mathcal{M}_d(\mathcal{K}, \mathcal{D}^*, \mathcal{D}^*) \cdot \frac{g\mathcal{D}^*\mathcal{D}^*\eta\theta_{\eta\pi^0}}{g\mathcal{D}^*\mathcal{D}^*\pi}, \quad (25)$$

$$i\mathcal{M}_e(\mathcal{D}^*, \mathcal{K}^*, \mathcal{K}^*, \eta) = i\mathcal{M}_e(\mathcal{D}^*, \mathcal{K}^*, \mathcal{K}^*) \cdot \frac{g\mathcal{K}^*\mathcal{K}^*\eta\theta_{\eta\pi^0}}{g\mathcal{K}^*\mathcal{K}^*\pi}, \quad i\mathcal{M}_e(\mathcal{K}^*, \mathcal{D}^*, \mathcal{D}^*, \eta) = i\mathcal{M}_e(\mathcal{K}^*, \mathcal{D}^*, \mathcal{D}^*) \cdot \frac{g\mathcal{D}^*\mathcal{D}^*\eta\theta_{\eta\pi^0}}{g\mathcal{D}^*\mathcal{D}^*\pi}. \quad (26)$$

As mentioned earlier, there does not exist a simple power counting in the framework of the effective Lagrangian approach. In order to show the relation between the tree and loop amplitudes, we take a typical loop amplitude, e.g. Fig. 2 (a), to demonstrate that it counts  $\mathcal{O}(m_\pi/m_3)$  with  $m_3$  the mass of the exchanged meson in the triangle loop. Since the masses of the intermediate  $D$  and final  $D_s$  are comparable, and the threshold of  $DK$  is about 253 MeV which is smaller than the masses of the exchanged mesons. By approximation we assume that the main contribution of the loop amplitude is from the kinematic region that the intermediate  $DK$  are nearly on shell and with a non-relativistic velocity  $v$ , while the exchanged mesons are highly off-shell with a small value of  $|t|$ . With the treatment  $1/(t - m_3^2) \simeq -1/m_3^2$  for the exchanged meson the loop amplitude scales as  $(v^5/v^4) \times p_\pi \cdot p_{D_s}/m_3^2 \simeq vE_{D_s}E_\pi/m_3^2$ . Taking into account the isospin breaking, the cancellation between these two isospin amplitudes scales as  $vE_{D_s}E_\pi(1/m_{K^{*\pm}}^2 - 1/m_{K^{*0}}^2) \simeq vE_\pi\delta_{K^*}/m_{K^*}^2 \simeq v(m_\pi/m_{K^*})(\delta_{K^*}/m_{K^*})$ , with  $\delta_{K^*} \equiv m_{K^{*0}} - m_{K^{*\pm}}$ . Although we do not include the coupling constants, the factor  $\delta_{K^*}/m_{K^*}$  represents the source of the isospin violation from the mass difference between the  $u$  and  $d$  quark. In contrast, the factor  $m_\pi/m_{K^*}$  indicates the suppression of the loop amplitudes of Fig. 2 (a) relative to the tree-level amplitude as a higher-order correction. Although the above analysis is qualitative, the numerical results with a reasonable cut-off for the ultra-violet (UV) divergence can provide a reliable estimate of the isospin-breaking corrections.

From the above amplitudes, we can obtain the total loop amplitude by summing up the contributions from the different loop diagrams. The decay  $D_s^{*+} \rightarrow D_s^+ \pi^0$  is a  $VPP$  type decay process, and we can always parametrize the total loop amplitude as

$$i\mathcal{M}_{\text{loop}} = ig_{\text{loop}}\varepsilon_{D_s^{*+}} \cdot (p_2 - p_3). \quad (27)$$

Taking into account the tree amplitude, the total decay amplitude can be expressed as

$$i\mathcal{M}_{D_s^{*+} \rightarrow D_s^+ \pi^0} = i(g_{\text{tree}} + g_{\text{loop}})\varepsilon_{D_s^{*+}} \cdot (p_{D_s^+} - p_{\pi^0}) \equiv ig_{\text{total}}\varepsilon_{D_s^{*+}} \cdot (p_{D_s^+} - p_{\pi^0}), \quad (28)$$

where  $g_{\text{total}}$  is the effective coupling for  $D_s^{*+} \rightarrow D_s^+ \pi^0$ . Then, the corresponding partial decay width is

$$\Gamma_{D_s^{*+} \rightarrow D_s^+ \pi^0} = \frac{|\mathbf{P}|^3 g_{\text{total}}^2}{6\pi M_V^2}. \quad (29)$$

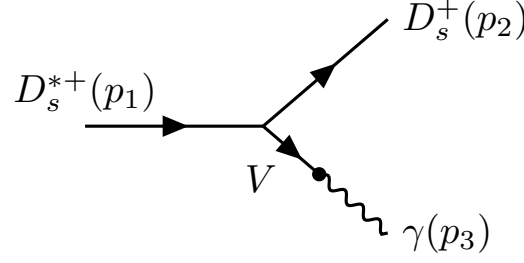
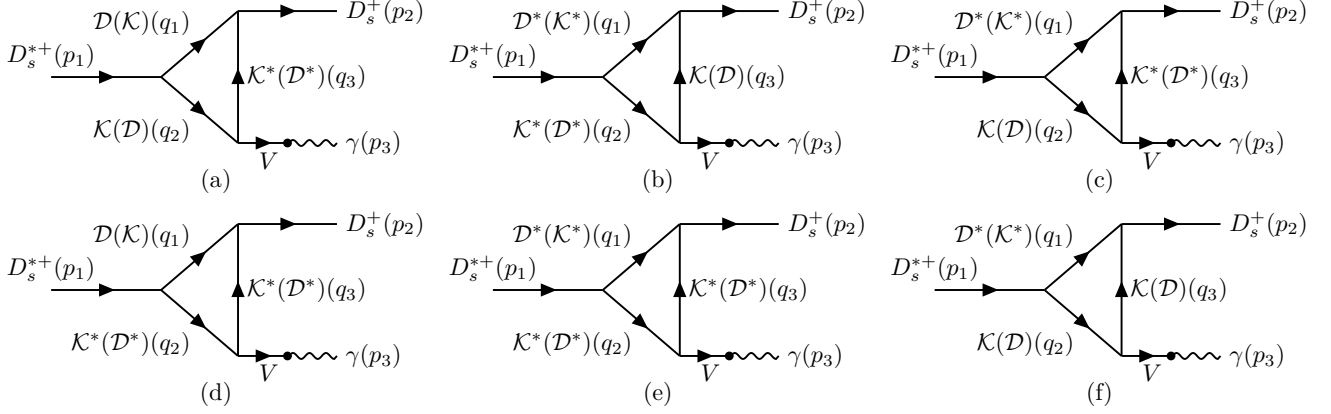
### C. Tree and loop amplitudes of $D_s^{*+} \rightarrow D_s^+ \gamma$ in the VMD model

Similar to the isospin-violating decay  $D_s^{*+} \rightarrow D_s^+ \pi^0$ , we can also calculate the radiative decay  $D_s^{*+} \rightarrow D_s^+ \gamma$ . The radiative decay can be described using the VMD model. The tree-level diagram is shown in Fig. 4. The tree-level amplitude for the process  $D_s^* \rightarrow D_s \gamma$  can be expressed as

$$i\mathcal{M}_{\text{tree}}^\gamma = ig_{\text{tree}}^\gamma(\gamma)\varepsilon_{\mu\nu\alpha\beta}p_1^\mu p_3^\nu \varepsilon_1^\alpha \varepsilon_3^\beta, \quad (30)$$

where  $g_{\text{tree}}^\gamma$  can be calculated using the VMD model,

$$g_{\text{tree}}^\gamma = ig_{D_s^* D_s V} \frac{em_V^2}{f_V} G_V \quad (31)$$

FIG. 4: Tree-level diagram of  $D_s^* \rightarrow D_s \gamma$  in the VMD model.FIG. 5: Schematic diagrams of the decay  $D_s^{*+} \rightarrow D_s^+ \gamma$  via intermediate meson loops in VMD model where  $V = \rho, \omega, \phi$ .

with

$$G_V \equiv \frac{-i}{p_\gamma^2 - m_V^2 + im_V \Gamma_V} = \frac{-i}{-m_V^2 + im_V \Gamma_V}. \quad (32)$$

In the above equations  $V = \rho, \omega, \phi$ , and  $e/f_V$  can be determined by experimental data of  $\Gamma_{V \rightarrow e^+ e^-}$ :

$$\frac{e}{f_V} = \left[ \frac{3\Gamma_{V \rightarrow e^+ e^-}}{2\alpha_e |\mathbf{p}_e|} \right]^{\frac{1}{2}} \quad (33)$$

where  $|\mathbf{p}_e|$  is the momentum of the final-state particle in the center-of-mass frame, and  $\alpha_e = \frac{1}{137}$  is the fine-structure constant. To match the coupling constants in HQEFT, we have

$$g_{D_s^* D_s V} = 4f_{D_s^* D_s V}. \quad (34)$$

For the tree level  $V = \phi, J/\psi$ , the coupling constant can be extracted:

$$g_{D_s^* D_s \gamma} = i \left( g_{D_s^* D_s \phi} \frac{em_\phi^2}{f_\phi} G_\phi + g_{D_s^* D_s \psi} \frac{em_\psi^2}{f_\psi} G_\psi \right), \quad (35)$$

with  $g_{D_s^* D_s \psi} = 2g_{J\psi D\bar{D}}/\tilde{M}$ ,  $\tilde{M} = \sqrt{M_{D_s^*} M_{D_s}}$  [27].

The schematic diagrams for the loop contributions are shown in Fig. 5. Similar to the process  $D_s^{*+} \rightarrow D_s^+ \pi^0$ , the corresponding amplitudes can be derived using the VMD model:

$$i\mathcal{M}_a(\mathcal{D}, \mathcal{K}, \mathcal{K}^*, \gamma) = \int \frac{d^4 q_3}{(2\pi)^4} \frac{g_{\mathcal{K}\mathcal{K}^* \gamma} g_{\mathcal{D}^* \mathcal{D} \mathcal{K}} g_{\mathcal{D}^* \mathcal{D} \mathcal{K}^*} q_2 \cdot \varepsilon^s(q_1 + p_2)_\alpha \left( g^{\alpha\beta} - \frac{q_3^\alpha q_3^\beta}{m_3^2} \right) \varepsilon_{\beta\sigma\mu\nu} \varepsilon_3^\sigma q_3^\mu p_3^\nu}{(q_1^2 - m_1^2)(q_2^2 - m_2^2)(q_3^2 - m_3^2)} \mathcal{F}(q_i^2), \quad (36)$$

$$i\mathcal{M}_a(\mathcal{K}, \mathcal{D}, \mathcal{D}^*, \gamma) = \int \frac{d^4 q_3}{(2\pi)^4} \frac{g_{\mathcal{D}^* \mathcal{D} \mathcal{K}} g_{\mathcal{D}^* \mathcal{D} \mathcal{K}} g_{\mathcal{D}^* \mathcal{D} \mathcal{K}} q_1 \cdot \varepsilon^s q_1^\mu \left( g_{\mu\nu} - \frac{q_{3\mu} q_{3\nu}}{m_3^2} \right) \varepsilon_{\nu\sigma\alpha\beta} \varepsilon_3^\sigma q_3^\alpha p_3^\beta}{(q_1^2 - m_1^2)(q_2^2 - m_2^2)(q_3^2 - m_3^2)} \mathcal{F}(q_i^2), \quad (37)$$



$$\begin{aligned}
i\mathcal{M}_b(\mathcal{D}^*, \mathcal{K}^*, \mathcal{K}, \gamma) &= \int \frac{d^4 q_3}{(2\pi)^4} \frac{g_{\mathcal{D}^* \mathcal{D}_s \mathcal{K}} g_{\mathcal{K}^* \mathcal{K} \gamma} (g_{\mathcal{D}_s^* \mathcal{D}^* \mathcal{K}^*} (p_1^\mu + q_1^\mu) g^{\alpha\beta} - 4f_{\mathcal{D}_s^* \mathcal{D}^* \mathcal{K}^*} (q_2^\beta g^{\alpha\mu} - q_2^\alpha g^{\beta\mu})) \varepsilon_\alpha^s q_3^\nu}{(q_1^2 - m_1^2)(q_2^2 - m_2^2)(q_3^2 - m_3^2)} \\
&\quad \times \varepsilon_{\lambda\sigma\kappa\rho} \varepsilon_3^\sigma q_3^\kappa p_3^\rho \left( g_{\beta\nu} - \frac{q_{1\beta} q_{1\nu}}{m_1^2} \right) \left( g_{\mu\lambda} - \frac{q_{2\mu} q_{2\lambda}}{m_2^2} \right) \mathcal{F}(q_i^2), \tag{38}
\end{aligned}$$

$$\begin{aligned}
i\mathcal{M}_b(\mathcal{K}^*, \mathcal{D}^*, \mathcal{D}, \gamma) &= - \int \frac{d^4 q_3}{(2\pi)^4} \frac{g_{\mathcal{D}_s \mathcal{D} \mathcal{K}^*} g_{\mathcal{D}^* \mathcal{D} \gamma} (g_{\mathcal{D}_s^* \mathcal{D}^* \mathcal{K}^*} (p_1^\mu + q_2^\mu) g^{\alpha\beta} - 4f_{\mathcal{D}_s^* \mathcal{D}^* \mathcal{K}^*} (q_1^\beta g^{\alpha\mu} - q_1^\alpha g^{\beta\mu})) \varepsilon_\alpha^s}{(q_1^2 - m_1^2)(q_2^2 - m_2^2)(q_3^2 - m_3^2)} \\
&\quad \times \varepsilon_{\lambda\sigma\kappa\rho} \varepsilon_3^\sigma q_3^\kappa p_3^\rho (p_2 + q_3)^\nu \left( g_{\beta\nu} - \frac{q_{1\beta} q_{1\nu}}{m_1^2} \right) \left( g_{\mu\lambda} - \frac{q_{2\mu} q_{2\lambda}}{m_2^2} \right) \mathcal{F}(q_i^2), \tag{39}
\end{aligned}$$

$$\begin{aligned}
i\mathcal{M}_c(\mathcal{D}^*, \mathcal{K}, \mathcal{K}^*, \gamma) &= - \int \frac{d^4 q_3}{(2\pi)^4} \frac{4g_{\mathcal{K} \mathcal{K}^* \gamma} f_{\mathcal{D}^* \mathcal{D}_s \mathcal{K}^*} g_{\mathcal{D}_s^* \mathcal{D}^* \mathcal{K}} \varepsilon_{\mu\nu\alpha\beta} p_1^\nu \varepsilon^{s\mu} q_1^\alpha \varepsilon_{\kappa\sigma\zeta\rho} q_3^\kappa p_2^\zeta}{(q_1^2 - m_1^2)(q_2^2 - m_2^2)(q_3^2 - m_3^2)} \\
&\quad \times \varepsilon_{\lambda\tau\kappa\rho} \varepsilon_3^\tau q_3^\kappa p_3^\rho \left( g^{\beta\rho} - \frac{q_1^\beta q_1^\rho}{m_1^2} \right) \left( g^{\sigma\lambda} - \frac{q_3^\sigma q_3^\lambda}{m_3^2} \right) \mathcal{F}(q_i^2), \tag{40}
\end{aligned}$$

$$\begin{aligned}
i\mathcal{M}_c(\mathcal{K}^*, \mathcal{D}, \mathcal{D}^*, \gamma) &= - \int \frac{d^4 q_3}{(2\pi)^4} \frac{16g_{\mathcal{D}^* \mathcal{D} \gamma} f_{\mathcal{D}^* \mathcal{D}_s \mathcal{K}^*} g_{\mathcal{D}_s^* \mathcal{D} \mathcal{K}^*} \varepsilon_{\alpha\beta\tau\mu} q_1^\alpha q_2^\tau \varepsilon^{s\mu} \varepsilon_{\kappa\rho\zeta\sigma} q_1^\kappa p_2^\zeta}{(q_1^2 - m_1^2)(q_2^2 - m_2^2)(q_3^2 - m_3^2)} \\
&\quad \times \varepsilon_{\lambda\tau\nu\delta} \varepsilon_3^\tau q_3^\nu p_3^\delta \left( g^{\beta\rho} - \frac{q_1^\beta q_1^\rho}{m_1^2} \right) \left( g^{\sigma\lambda} - \frac{q_3^\sigma q_3^\lambda}{m_3^2} \right) \mathcal{F}(q_i^2), \tag{41}
\end{aligned}$$

$$\begin{aligned}
i\mathcal{M}_d(\mathcal{D}, \mathcal{K}^*, \mathcal{K}^*, \gamma) &= \int \frac{d^4 q_3}{(2\pi)^4} \frac{4g_{\mathcal{K} \mathcal{K}^* \gamma} g_{\mathcal{D} \mathcal{D}_s \mathcal{K}^*} f_{\mathcal{D}_s^* \mathcal{D} \mathcal{K}^*} \varepsilon_{\alpha\beta\tau\mu} q_2^\alpha q_1^\tau \varepsilon^{s\mu} (q_1 + p_2)_\sigma}{(q_1^2 - m_1^2)(q_2^2 - m_2^2)(q_3^2 - m_3^2)} \\
&\quad \times (\varepsilon_{3\rho} p_{3\lambda} - \varepsilon_{3\lambda} p_{3\rho}) \left( g^{\beta\rho} - \frac{q_2^\beta q_2^\rho}{m_2^2} \right) \left( g^{\sigma\lambda} - \frac{q_3^\sigma q_3^\lambda}{m_3^2} \right) \mathcal{F}(q_i^2), \tag{42}
\end{aligned}$$

$$\begin{aligned}
i\mathcal{M}_d(\mathcal{K}, \mathcal{D}^*, \mathcal{D}^*, \gamma) &= - \int \frac{d^4 q_3}{(2\pi)^4} \frac{g_{\mathcal{D}_s^* \mathcal{D}^* \mathcal{K}} g_{\mathcal{D}^* \mathcal{D}_s \mathcal{K}} (g_{\mathcal{D}^* \mathcal{D}^* \gamma} (q_2 + p_3) \cdot \varepsilon_3 g_{\rho\lambda} - f_{\mathcal{D}^* \mathcal{D}^* \gamma} (\varepsilon_{3\rho} p_{3\lambda} - \varepsilon_{3\lambda} p_{3\rho}))}{(q_1^2 - m_1^2)(q_2^2 - m_2^2)(q_3^2 - m_3^2)} \\
&\quad \times \varepsilon_{\mu\nu\alpha\beta} p_1^\nu \varepsilon^{s\mu} q_2^\alpha q_1^\beta \left( g^{\beta\rho} - \frac{q_2^\beta q_2^\rho}{m_2^2} \right) \left( g^{\sigma\lambda} - \frac{q_3^\sigma q_3^\lambda}{m_3^2} \right) \mathcal{F}(q_i^2), \tag{43}
\end{aligned}$$

$$\begin{aligned}
i\mathcal{M}_e(\mathcal{D}^*, \mathcal{K}^*, \mathcal{K}^*, \gamma) &= \int \frac{d^4 q_3}{(2\pi)^4} \frac{4(g_{\mathcal{D}_s^* \mathcal{D}^* \mathcal{K}^*} (p_1 + q_1)_\mu g_{\alpha\beta} - 4f_{\mathcal{D}_s^* \mathcal{D}^* \mathcal{K}^*} (q_2\beta g_{\alpha\mu} - q_2\alpha g_{\beta\mu})) \varepsilon^{s\alpha}}{(q_1^2 - m_1^2)(q_2^2 - m_2^2)(q_3^2 - m_3^2)} \\
&\quad \times f_{\mathcal{D}^* \mathcal{D}_s \mathcal{K}^*} \varepsilon_{\kappa\sigma\zeta\rho} q_3^\kappa p_2^\zeta g_{\mathcal{K} \mathcal{K}^* \gamma} (\varepsilon_{3\nu} p_{3\lambda} - \varepsilon_{3\lambda} p_{3\nu}) \\
&\quad \times \left( g^{\beta\rho} - \frac{q_1^\beta q_1^\rho}{m_1^2} \right) \left( g^{\mu\nu} - \frac{q_2^\mu q_2^\nu}{m_2^2} \right) \left( g^{\sigma\lambda} - \frac{q_3^\sigma q_3^\lambda}{m_3^2} \right) \mathcal{F}(q_i^2), \tag{44}
\end{aligned}$$

$$\begin{aligned}
i\mathcal{M}_e(\mathcal{K}^*, \mathcal{D}^*, \mathcal{D}^*, \gamma) &= \int \frac{d^4 q_3}{(2\pi)^4} \frac{4f_{\mathcal{D}^* \mathcal{D}_s \mathcal{K}^*} (g_{\mathcal{D}_s^* \mathcal{D}^* \mathcal{K}^*} (p_1 + q_2)_\beta g_{\alpha\mu} - 4f_{\mathcal{D}_s^* \mathcal{D}^* \mathcal{K}^*} (q_{1\mu} g_{\alpha\beta} - q_{1\alpha} g_{\beta\mu})) \varepsilon^{s\alpha}}{(q_1^2 - m_1^2)(q_2^2 - m_2^2)(q_3^2 - m_3^2)} \\
&\quad \times \varepsilon_{\kappa\rho\zeta\sigma} q_1^\kappa p_2^\zeta (g_{\mathcal{D}^* \mathcal{D}^* \gamma} (q_2 + p_3) \cdot \varepsilon_3 g_{\nu\lambda} - f_{\mathcal{D}^* \mathcal{D}^* \gamma} (\varepsilon_{3\nu} p_{3\lambda} - \varepsilon_{3\lambda} p_{3\nu})) \\
&\quad \times \left( g^{\beta\rho} - \frac{q_1^\beta q_1^\rho}{m_1^2} \right) \left( g^{\mu\nu} - \frac{q_2^\mu q_2^\nu}{m_2^2} \right) \left( g^{\sigma\lambda} - \frac{q_3^\sigma q_3^\lambda}{m_3^2} \right) \mathcal{F}(q_i^2). \tag{45}
\end{aligned}$$

$$i\mathcal{M}_f(\mathcal{D}^*, \mathcal{K}, \mathcal{K}, \gamma) = - \int \frac{d^4 q_3}{(2\pi)^4} \frac{g_{\mathcal{D}_s^* \mathcal{D}^* \mathcal{K}} g_{\mathcal{D}^* \mathcal{D} \mathcal{K}} g_{\mathcal{K} \mathcal{K} \gamma} \varepsilon_{\mu\nu\alpha\beta} p_1^\nu \varepsilon^{s\mu} q_1^\alpha p_2^\beta \varepsilon_3 \cdot (q_2 + q_3) \left( g^{\beta\rho} - \frac{q_1^\beta q_1^\rho}{m_1^2} \right)}{(q_1^2 - m_1^2)(q_2^2 - m_2^2)(q_3^2 - m_3^2)} \mathcal{F}(q_i^2), \tag{46}$$

$$i\mathcal{M}_f(\mathcal{K}^*, \mathcal{D}, \mathcal{D}, \gamma) = - \int \frac{d^4 q_3}{(2\pi)^4} \frac{4f_{\mathcal{D}_s^* \mathcal{D} \mathcal{K}^*} g_{\mathcal{D} \mathcal{D} \mathcal{K}^*} g_{\mathcal{D} \mathcal{D} \gamma} \varepsilon_{\alpha\beta\tau\mu} q_1^\alpha q_2^\tau \varepsilon^{s\mu} (q_1 + p_2)_\rho \varepsilon_3 \cdot (q_2 + q_3) \left( g^{\beta\rho} - \frac{q_1^\beta q_1^\rho}{m_1^2} \right)}{(q_1^2 - m_1^2)(q_2^2 - m_2^2)(q_3^2 - m_3^2)} \mathcal{F}(q_i^2). \tag{47}$$

In the above equations the corresponding radiative decay coupling constants can be calculated using the VMD model [31], the same form factor as Eq. (21) is adopted. The relevant expressions are as follows:

$$g_{K^+ K^+ \gamma} = i(g_{\rho^0 K^+ K} - \frac{em_{\rho^0}^2}{f_{\rho^0}} G_{\rho^0} + g_{\omega K^+ K} - \frac{em_{\omega}^2}{f_{\omega}} G_{\omega} + g_{\phi K^+ K} - \frac{em_{\phi}^2}{f_{\phi}} R G_{\phi}), \tag{48}$$



$$g_{K^0 K^{*0} \gamma} = i(g_{\rho^0 K^{*0} \bar{K}^{*0}} \frac{em_{\rho^0}^2}{f_{\rho^0}} G_{\rho^0} + g_{\omega K^{*0} \bar{K}^{*0}} \frac{em_{\omega}^2}{f_{\omega}} G_{\omega} + g_{\phi K^{*0} \bar{K}^{*0}} \frac{em_{\phi}^2}{f_{\phi}} RG_{\phi}), \quad (49)$$

$$g_{D^{*0} D^0 \gamma} = i(g_{\rho^0 D^{*0} \bar{D}^0} \frac{em_{\rho^0}^2}{f_{\rho^0}} G_{\rho^0} + g_{\omega D^{*0} \bar{D}^0} \frac{em_{\omega}^2}{f_{\omega}} G_{\omega} + g_{\phi D^{*0} \bar{D}^0} \frac{em_{\phi}^2}{f_{\phi}} RG_{\phi}), \quad (50)$$

$$g_{D^{*+} D^+ \gamma} = i(g_{\rho^0 D^{*+} D^-} \frac{em_{\rho^0}^2}{f_{\rho^0}} G_{\rho^0} + g_{\omega D^{*+} D^-} \frac{em_{\omega}^2}{f_{\omega}} G_{\omega} + g_{\phi D^{*+} D^-} \frac{em_{\phi}^2}{f_{\phi}} RG_{\phi}), \quad (51)$$

$$g_{K^{*+} K^{*+} \gamma} = i(g_{\rho^0 K^{*+} K^{*-}} \frac{em_{\rho^0}^2}{f_{\rho^0}} G_{\rho^0} + g_{\omega K^{*+} K^{*-}} \frac{em_{\omega}^2}{f_{\omega}} G_{\omega} + g_{\phi K^{*+} K^{*-}} \frac{em_{\phi}^2}{f_{\phi}} RG_{\phi}), \quad (52)$$

$$g_{K^{*0} K^{*0} \gamma} = i(g_{\rho^0 K^{*0} \bar{K}^{*0}} \frac{em_{\rho^0}^2}{f_{\rho^0}} G_{\rho^0} + g_{\omega K^{*0} \bar{K}^{*0}} \frac{em_{\omega}^2}{f_{\omega}} G_{\omega} + g_{\phi K^{*0} \bar{K}^{*0}} \frac{em_{\phi}^2}{f_{\phi}} RG_{\phi}), \quad (53)$$

$$g_{D^{*0} D^{*0} \gamma} = i(g_{\rho^0 D^{*0} D^{*0}} \frac{em_{\rho^0}^2}{f_{\rho^0}} G_{\rho^0} + g_{\omega D^{*0} D^{*0}} \frac{em_{\omega}^2}{f_{\omega}} G_{\omega} + g_{\phi D^{*0} D^{*0}} \frac{em_{\phi}^2}{f_{\phi}} RG_{\phi}), \quad (54)$$

$$f_{D^{*0} D^{*0} \gamma} = 4i(f_{\rho^0 D^{*0} D^{*0}} \frac{em_{\rho^0}^2}{f_{\rho^0}} G_{\rho^0} + f_{\omega D^{*0} D^{*0}} \frac{em_{\omega}^2}{f_{\omega}} G_{\omega} + f_{\phi D^{*0} D^{*0}} \frac{em_{\phi}^2}{f_{\phi}} RG_{\phi}), \quad (55)$$

$$g_{D^{*+} D^{*+} \gamma} = i(g_{\rho^0 D^{*+} D^{*-}} \frac{em_{\rho^0}^2}{f_{\rho^0}} G_{\rho^0} + g_{\omega D^{*+} D^{*-}} \frac{em_{\omega}^2}{f_{\omega}} G_{\omega} + g_{\phi D^{*+} D^{*-}} \frac{em_{\phi}^2}{f_{\phi}} RG_{\phi}), \quad (56)$$

$$f_{D^{*+} D^{*+} \gamma} = 4i(f_{\rho^0 D^{*+} D^{*-}} \frac{em_{\rho^0}^2}{f_{\rho^0}} G_{\rho^0} + f_{\omega D^{*+} D^{*-}} \frac{em_{\omega}^2}{f_{\omega}} G_{\omega} + f_{\phi D^{*+} D^{*-}} \frac{em_{\phi}^2}{f_{\phi}} RG_{\phi}), \quad (57)$$

$$g_{K^+ K^+ \gamma} = i(g_{\rho^0 K^+ K^-} \frac{em_{\rho^0}^2}{f_{\rho^0}} G_{\rho^0} + g_{\omega K^+ K^-} \frac{em_{\omega}^2}{f_{\omega}} G_{\omega} + g_{\phi K^+ K^-} \frac{em_{\phi}^2}{f_{\phi}} RG_{\phi}), \quad (58)$$

$$g_{K^0 K^0 \gamma} = i(g_{\rho^0 K^0 \bar{K}^0} \frac{em_{\rho^0}^2}{f_{\rho^0}} G_{\rho^0} + g_{\omega K^0 \bar{K}^0} \frac{em_{\omega}^2}{f_{\omega}} G_{\omega} + g_{\phi K^0 \bar{K}^0} \frac{em_{\phi}^2}{f_{\phi}} RG_{\phi}), \quad (59)$$

$$g_{D^+ D^+ \gamma} = i(g_{\rho^0 D^+ D^-} \frac{em_{\rho^0}^2}{f_{\rho^0}} G_{\rho^0} + g_{\omega D^+ D^-} \frac{em_{\omega}^2}{f_{\omega}} G_{\omega} + g_{\phi D^+ D^-} \frac{em_{\phi}^2}{f_{\phi}} RG_{\phi}), \quad (60)$$

$$g_{D^0 D^0 \gamma} = i(g_{\rho^0 D^0 \bar{D}^0} \frac{em_{\rho^0}^2}{f_{\rho^0}} G_{\rho^0} + g_{\omega D^0 \bar{D}^0} \frac{em_{\omega}^2}{f_{\omega}} G_{\omega} + g_{\phi D^0 \bar{D}^0} \frac{em_{\phi}^2}{f_{\phi}} RG_{\phi}), \quad (61)$$

where  $R = 0.8$  is the  $SU(3)$  flavor symmetry breaking parameter for processes involving the strange  $s$  quark.

In addition to the contributions from Fig. 5, we also need to consider the contributions from the contact diagrams shown in Fig. 6, which are induced by the requirement of Lorentz gauge invariance for the EM transitions. Similar to what found in Ref. [36], we confirm that Figs. 6(b)-(d), do not contribute to the amplitude, as the integrals involve odd powers of momentum after the Feynman parameterization. Consequently, only Fig. 6(a) has non-vanishing contributions to the amplitude.

The corresponding amplitudes arising from Fig. 6(a) have the following expressions:

$$i\mathcal{M}_a(\mathcal{D}^*, \mathcal{K}, \gamma) = - \int \frac{d^4 q_3}{(2\pi)^4} \frac{g_{\mathcal{D}^* \mathcal{D}_s \mathcal{K}} g_{\mathcal{D}_s^* \mathcal{D}^* \mathcal{K}} \varepsilon_{\mu\nu\alpha\beta} \varepsilon^{s\mu} (p_1^\nu \varepsilon_3^\alpha + \varepsilon_3^\nu q_1^\alpha) p_2^\rho}{(q_1^2 - m_1^2)(q_2^2 - m_2^2)} \left( g^{\beta\rho} - \frac{q_1^\beta q_1^\rho}{m_1^2} \right) \mathcal{F}(q_i^2), \quad (62)$$

$$i\mathcal{M}_a(\mathcal{K}^*, \mathcal{D}, \gamma) = - \int \frac{d^4 q_3}{(2\pi)^4} \frac{4g_{\mathcal{D} \mathcal{D}_s \mathcal{K}^*} f_{\mathcal{D}_s^* \mathcal{D} \mathcal{K}^*} \varepsilon_{\mu\nu\alpha\beta} \varepsilon^{s\mu} (p_1^\nu \varepsilon_3^\alpha + \varepsilon_3^\nu q_1^\alpha) (p_2 + q_2)^\rho}{(q_1^2 - m_1^2)(q_2^2 - m_2^2)} \left( g^{\beta\rho} - \frac{q_1^\beta q_1^\rho}{m_1^2} \right) \mathcal{F}(q_i^2), \quad (63)$$

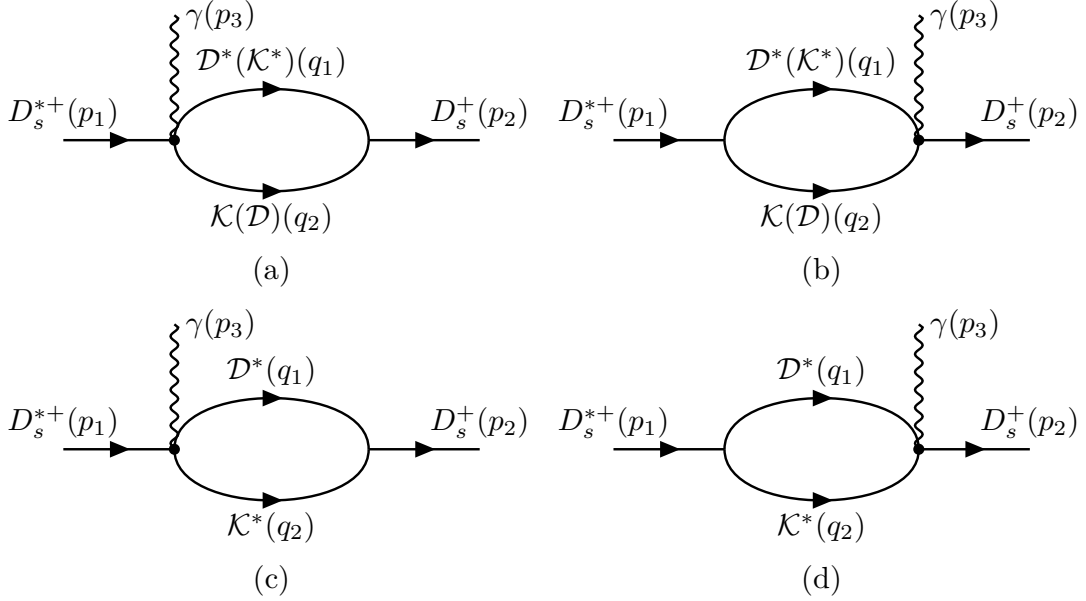
where the same form factor as Eq. (21) is adopted.

From the above amplitudes, we can obtain the total radiative decay loop amplitude by summing up the contributions from the different loop diagrams. The decay  $D_s^{*+} \rightarrow D_s^+ \gamma$  is a  $VVP$  type decay process, and we can always parametrize the total loop amplitude as

$$i\mathcal{M}_{\text{loop}}^\gamma = ig_{\text{loop}}^\gamma \varepsilon_{\mu\nu\alpha\beta} p_1^\mu p_3^\nu \varepsilon_1^\alpha \varepsilon_3^\beta \quad (64)$$

Taking into account the tree amplitude, the total decay amplitude can be expressed as

$$i\mathcal{M}_{D_s^{*+} \rightarrow D_s^+ \gamma} = i(g_{\text{tree}}^\gamma + g_{\text{loop}}^\gamma) \varepsilon_{\mu\nu\alpha\beta} p_1^\mu p_3^\nu \varepsilon_1^\alpha \varepsilon_3^\beta \equiv ig_{\text{total}}^\gamma \varepsilon_{D_s^{*+}} \cdot (p_{D_s^+} - p_{\pi^0}), \quad (65)$$

FIG. 6: Contact diagrams of the decay  $D_s^{*+} \rightarrow D_s^+ \gamma$ .

where  $g_{\text{total}}^\gamma$  is the effective coupling for  $D_s^{*+} \rightarrow D_s^+ \gamma$ . Then, the corresponding partial decay width is

$$\Gamma_{D_s^{*+} \rightarrow D_s^+ \gamma} = \frac{|\mathbf{p}|^3 (g_{\text{total}}^\gamma)^2}{12\pi}. \quad (66)$$

### III. NUMERICAL RESULTS AND DISCUSSIONS

Proceeding to the numerical calculations of the tree-level and loop contributions for  $D_s^{*+} \rightarrow D_s^+ \pi^0$  and  $D_s^{*+} \rightarrow D_s^+ \gamma$ , those common coupling constants are listed in Tables I-IV, with the relative phases determined by SU(4) flavor symmetry. This advantage allows us to combine these two decay processes together, and investigate the experimental constraint on the range of the only individual parameter  $g_{J/\psi D \bar{D}}$  in  $D_s^{*+} \rightarrow D_s^+ \gamma$ . Note that the same form factor is introduced in the loop integrals. We can also investigate the dependence of the branching ratio fraction between these two decay channels on the cut-off parameter. The masses of the relevant particles are taken from the PDG [28].

TABLE I: The values of the  $VPP$  coupling constants.

Coupling Constant	$g_{D_s^{*+} D^0 K}$	$g_{D_s^+ D^0 K^*}$	$g_{D^{*0} D^0 \pi}$	$g_{D^{*-} D^+ \pi}$	$g_{D_s^{*+} D^+ K}$	$g_{D^{*0} D_s^+ K}$	$g_{D_s^+ D^+ K^*}$	$g_{D^{*+} D_s^+ K}$	$g_{VPP}$
Numerical Value	18.40	3.84	17.29	-17.33	18.42	17.77	3.84	17.78	4.18

TABLE II: The values of the  $VVP$  coupling constants.

Coupling Constant	$g_{D_s^{*+} D^{*0} K}$	$f_{D^{*0} D_s^+ K^*}$	$f_{D_s^+ D^0 K^*}$	$g_{D^{*0} \bar{D}^0 \pi^0}$	$g_{D^{*+} D^* - \pi^0}$	$g_{VVP}$
Numerical Value(GeV <sup>-1</sup> )	7.81	2.38	2.47	8.94	-8.94	7.93

In Table V we list the calculation results of  $D_s^{*+} \rightarrow D_s^+ \pi_0$  for the tree, loop transitions and the total, respectively, with five typical cut-off parameter values  $\alpha = 1.0, 1.35, 1.5, 1.65$  and  $2.0$ . We can see that although there exist some sensitivities of the loop contribution to the cutoff parameter  $\alpha$ , the loop contributions turn out to be rather stable. Combining the tree and loop amplitudes together, the partial decay width reads  $\Gamma_{\text{total}} = 9.92_{-0.66}^{+0.76}$  eV in the range of  $\alpha = 1.5 \pm 0.15$ , which serves as a reasonable estimate of the model uncertainties in our theoretical calculations. Similar to what found in Ref. [17] that the small higher-order corrections can introduce rather significant interferences in the final results, we also find that the loop contributions cannot be neglected.

TABLE III: The values of the  $VVV$  coupling constants.

Coupling Constant	$g_{VVV}$	$g_{D_s^{*+}D^*0K^*}$	$f_{D_s^*D^*0K^*}$
Numerical Value	4.47	3.83	4.79

TABLE IV: The values of the electromagnetic coupling constants in VMD model.

Coupling Constant	$g_{K^{*+}K^+\gamma}$	$g_{K^*0K^0\gamma}$	$g_{D^*0D^0\gamma}$	$g_{D^{*+}D^+\gamma}$
Numerical Value(GeV $^{-1}$ )	$-0.288 + 0.063i$	$0.369 + 0.062i$	$-0.383 - 0.082i$	$0.492 + 0.082i$
Coupling Constant	$g_{K^{*+}K^+\gamma}$	$g_{K^*0K^0\gamma}$	$g_{D^*0D^0\gamma}(f_{D^*0D^0\gamma})$	$g_{D^{*+}D^+\gamma}(f_{D^{*+}D^+\gamma})$
Numerical Value	$-0.162 - 0.035i$	$0.208 + 0.034i$	$-0.139 - 0.031i(-0.695 - 0.152i)$	$0.178 + 0.030i(0.892 + 0.150i)$
Coupling Constant	$g_{K^+K^+\gamma}$	$g_{K^0K^0\gamma}$	$g_{D^0D^0\gamma}$	$g_{D^+D^+\gamma}$
Numerical Value	$-0.288 + 0.063i$	$0.369 + 0.062i$	$-0.383 - 0.082i$	$0.492 + 0.082i$

TABLE V: Contributions of the tree diagram, loop diagrams, and the combination of tree and loop diagrams to the partial decay width of  $D_s^{*+} \rightarrow D_s^+\pi^0$  with  $\alpha = 1.0, 1.35, 1.5, 1.65$  and  $2.0$  in unit of eV.

$\alpha$	1.0	1.35	1.5	1.65	2.0
$\Gamma_{\text{tree}}$	6.93	6.93	6.93	6.93	6.93
$\Gamma_{\text{loop}}$	0.04	0.17	0.26	0.41	0.90
$\Gamma_{\text{total}}$	8.07	9.26	9.92	10.67	12.81

In Table VI we compare our result with other theoretical calculations, i.e. the covariant model (CM) [13] and the chiral perturbation theory ( $\chi$ PT) [17]. It shows that Our result is consistent with that obtained from  $\chi$ PT [17]. Note that the results from the CM [13] are significantly larger than both our result and the  $\chi$ PT calculation [17].

TABLE VI: Comparisons of the partial decay width of  $D_s^{*+} \rightarrow D_s^+\pi^0$ . The decay widths are in the units of eV. The uncertainties of our result are given by  $\alpha = 1.5 \pm 0.15$ .

	CM [13]	$\chi$ PT [17]	Our work
$\Gamma(D_s^{*+} \rightarrow D_s^+\pi^0)$	$277_{-26}^{+28}$	$8.1_{-2.6}^{+3.0}$	$9.92_{-0.66}^{+0.76}$

To see more clearly the role played by the intermediate loop transitions, we plot the dependence of the decay width of  $D_s^{*+} \rightarrow D_s^+\pi^0$  on the cut-off parameter  $\alpha$ , which includes contributions from tree diagrams, loop diagrams, and the sum of tree and loop diagrams, as shown in Fig. 7. It should be noted that the contributions from the intermediate meson loops are cumulative, with different channels contributing comparably. The channel involving the exchange of  $\mathcal{K}$ , i.e. the  $(D^*, \mathcal{K}^*, \mathcal{K})$  channel, has a relatively larger contribution, approximately twice of the other channels. To better illustrate the cumulative effect, we plot the exclusive contribution of this channel in Fig. 7. As shown there, this relatively dominant loop transition only contributes a small portion of the total width.

As discussed earlier, the transitions  $D_s^{*+} \rightarrow D_s^+\pi^0$  and  $D_s^{*+} \rightarrow D_s^+\gamma$  share the same strong couplings except for  $g_{J/\psi D\bar{D}}$  which appears in the tree amplitude of  $D_s^{*+} \rightarrow D_s^+\gamma$ . In the literature one finds that this coupling takes values in a range of  $g_{J/\psi D\bar{D}} = 7 \sim 7.5$  [27, 37–40]. As we will show later that the loop correction in  $D_s^{*+} \rightarrow D_s^+\gamma$  is negligibly small, it thus allows us to conclude that the main uncertainty source in this combined analysis should come from the tree-level contribution, i.e. the uncertainty of  $g_{J/\psi D\bar{D}}$ .

Our strategy below is to first constrain the coupling  $g_{J/\psi D\bar{D}}$  using the experimental data for the branching ratio fraction of  $D_s^{*+} \rightarrow D_s^+\pi^0$  to  $D_s^{*+} \rightarrow D_s^+\gamma$  [28, 41]. We then constrain  $g_{J/\psi D\bar{D}}$  by assuming that this coupling is the only adjustable parameter for reproducing the branching ratio fraction with the cut-off parameter  $\alpha = 1.5$ , while all the other common couplings are fixed by  $D_s^{*+} \rightarrow D_s^+\pi^0$ . With the branching ratio fraction data from the PDG [28] we extract:

$$g_{J\psi D\bar{D}} = 7.23 \pm 0.06. \quad (67)$$

This value is within the range of  $g_{J/\psi D\bar{D}} = 7 \sim 7.5$  adopted in the literature [27, 37–40], but is better constrained.

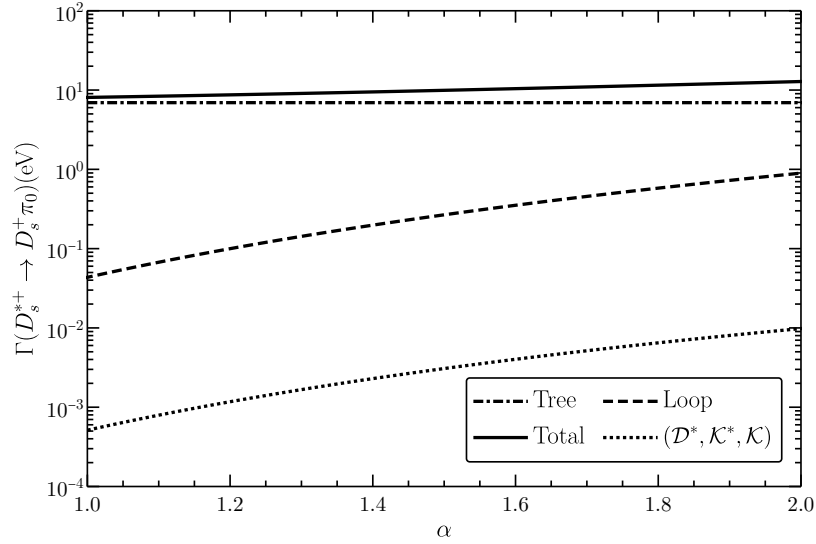


FIG. 7: The partial decay width of  $D_s^{*+} \rightarrow D_s^+ \pi^0$  is shown as a function of the cut-off parameter  $\alpha$ . The solid curve illustrates the total contribution, the dot-dashed curve indicates the tree-level contribution, and the dashed curve shows the loop contributions. The dotted curve depicts the contribution from the  $(D^*, \mathcal{K}^*, \mathcal{K})$  loop as a demonstration of the contribution from a single process.

TABLE VII: Experimentally measured branching ratios and relative branching ratios of  $D_s^{*+} \rightarrow D_s^+ \pi^0$  and  $D_s^{*+} \rightarrow D_s^+ \gamma$ .

	$\text{BR}(D_s^{*+} \rightarrow D_s^+ \gamma)$	$\text{BR}(D_s^{*+} \rightarrow D_s^+ \pi^0)$	$\text{BR}(D_s^{*+} \rightarrow D_s^+ \pi^0)/\text{BR}(D_s^{*+} \rightarrow D_s^+ \gamma)$
PDG [28]	$(93.6 \pm 0.4)\%$	$(5.77 \pm 0.35)\%$	$(6.2 \pm 0.4)\%$
BESIII [41]	$(93.54 \pm 0.38 \pm 0.22)\%$	$(5.76 \pm 0.38 \pm 0.16)\%$	$(6.16 \pm 0.43 \pm 0.18)\%$

TABLE VIII: The partial decay width of  $D_s^{*+} \rightarrow D_s^+ \gamma$  and the total width of  $D_s^{*+}$  obtained using the experimentally measured relative branching ratio and the calculated width of  $D_s^{*+} \rightarrow D_s^+ \pi^0$  with  $\alpha = 1.5$ .

	$\Gamma(D_s^{*+} \rightarrow D_s^+ \gamma)$	$\Gamma_{\text{total}}(D_s^{*+})$
PDG [28]	$160_{-10}^{+10} \text{eV}$	$172_{-10}^{+10} \text{eV}$
BESIII [41]	$161_{-16}^{+16} \text{eV}$	$172_{-16}^{+16} \text{eV}$

TABLE IX: Contributions of the tree diagram, loop diagrams, and the combination of tree and loop diagrams to the partial decay width of  $D_s^{*+} \rightarrow D_s^+ \gamma$  with  $\alpha = 1.0, 1.35, 1.5, 1.65$  and  $2.0$  in unit of eV and  $g_{J/\psi D \bar{D}} = 7.23$ .

$\alpha$	1.0	1.35	1.5	1.65	2.0
$\Gamma_{\text{tree}}$	153.89	153.89	153.89	153.89	153.89
$\Gamma_{\text{loop}}$	0.54	2.22	3.59	5.55	13.14
$\Gamma_{\text{total}}$	155.30	157.84	159.69	162.16	171.15

TABLE X: The partial decay widths of  $D_s^{*+} \rightarrow D_s^+ \pi^0$  and  $D_s^{*+} \rightarrow D_s^+ \gamma$ , as well as the total width of  $D_s^{*+}$  as the sum of both, for  $\alpha = 1.5 \pm 0.15$  with  $g_{J/\psi D \bar{D}}$  fixed at 7.23, and for  $g_{J/\psi D \bar{D}} = 7.23 \pm 0.06$ .

	$\Gamma(D_s^{*+} \rightarrow D_s^+ \pi^0)$	$\Gamma(D_s^{*+} \rightarrow D_s^+ \gamma)$	$\Gamma_{\text{total}}(D_s^{*+})$
$\alpha = 1.5 \pm 0.15, g_{J/\psi D \bar{D}} = 7.23$	$9.92_{-0.66}^{+0.76}$	$159.7_{-1.8}^{+2.5}$	$169.6_{-2.0}^{+2.6}$
$\alpha = 1.5 \pm 0.15, g_{J/\psi D \bar{D}} = 7.23 \pm 0.06$	$9.92_{-0.66}^{+0.76}$	$160_{-12}^{+13}$	$170_{-12}^{+13}$

It is necessary to examine the magnitude of the loop corrections for  $D_s^* \rightarrow D_s \gamma$  and its sensitivity to the cut-off parameter  $\alpha$ . In Table IX, we list the calculated partial decay widths of  $D_s^* \rightarrow D_s \gamma$  for the tree-level, loop

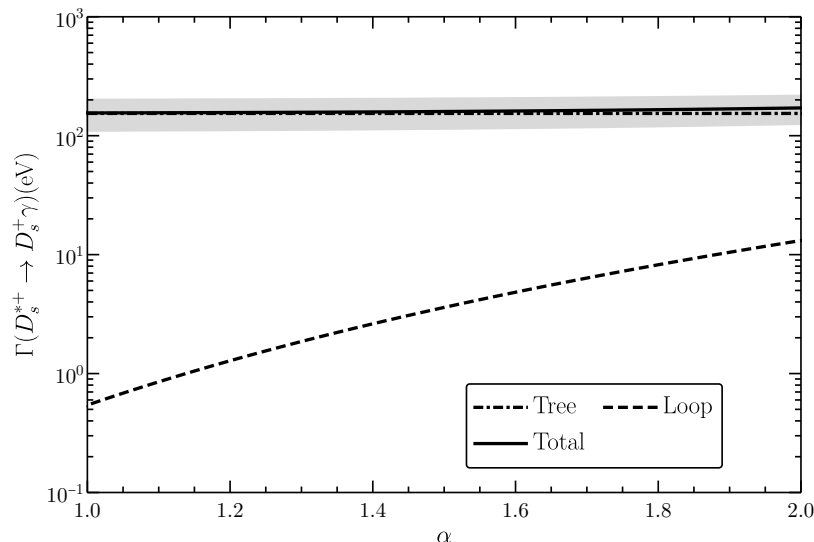


FIG. 8: The partial decay width of  $D_s^{*+} \rightarrow D_s^+ \gamma$  is shown as a function of the cut-off parameter  $\alpha$  with  $g_{J/\psi D \bar{D}} = 7.23$ . The solid curve illustrates the total contribution, the dot-dashed curve indicates the tree-level contribution, and the dashed curve shows the loop contributions. The light gray band represents the variation range of the results for  $g_{J/\psi D \bar{D}} = 7 \sim 7.5$ .

contributions, and the total, with five typical cut-off parameter values  $\alpha = 1.0, 1.35, 1.5, 1.65, \text{ and } 2.0$ , and  $g_{J/\psi D \bar{D}} = 7.23$ . In Fig. 8, we plot the cut-off dependence of the partial decay width of  $D_s^{*+} \rightarrow D_s^+ \gamma$ , as well as the variation range of the results for  $g_{J/\psi D \bar{D}} = 7 \sim 7.5$ . In contrast with the  $D_s^* \rightarrow D_s \pi^0$  decay channel, the loop corrections to the tree-level amplitude are negligibly small. The uncertainty in the calculation of the partial width for  $D_s^* \rightarrow D_s \gamma$  is predominantly determined by the tree-level contributions. The error in the tree-level contributions mainly arises from the uncertainty of  $g_{J/\psi D \bar{D}}$ . Notice that within the range  $g_{J/\psi D \bar{D}} = 7 \sim 7.5$ , the partial width of  $D_s^* \rightarrow D_s \gamma$  varies approximately between  $100 \sim 200$  eV, which encompasses the result estimated using the decay width of  $D_s^* \rightarrow D_s \pi^0$ . This can be regarded as a self-consistency check of the formalism.

To examine the dependence of the partial decay width and total width of  $D_s^{*+}$  on the cut-off parameter  $\alpha$  and the coupling constant  $g_{J/\psi D \bar{D}}$ , we present in Table X the partial decay widths of  $D_s^{*+} \rightarrow D_s^+ \pi^0$  and  $D_s^{*+} \rightarrow D_s^+ \gamma$ , as well as the total width of  $D_s^{*+}$  as the sum of both, for  $\alpha = 1.5 \pm 0.15$  with  $g_{J/\psi D \bar{D}}$  fixed at 7.23, and for  $g_{J/\psi D \bar{D}} = 7.23 \pm 0.06$ , respectively. Note that  $\Gamma(D_s^{*+} \rightarrow D_s^+ \pi^0)$  does not depend on  $g_{J/\psi D \bar{D}}$ . The variation of  $g_{J/\psi D \bar{D}}$  will only bring errors to  $\Gamma(D_s^{*+} \rightarrow D_s^+ \gamma)$ , and this absorbs the primary uncertainties for the estimate of the total width.

It should be stressed that our formalism provides a relatively stringent constraint on the coupling  $g_{J/\psi D \bar{D}}$  which results in an improved estimate of the total width. Recalling that the range of  $g_{J/\psi D \bar{D}} = 7 \sim 7.5$  is adopted in the literature [27, 37–40], with such a large uncertainty for  $g_{J/\psi D \bar{D}}$ , the uncertainties with the total width can amount to more than 20%. In this sense we may regard that the decay of  $D_s^*$  can provide a reliable constraint on the coupling  $g_{J/\psi D \bar{D}}$ .

#### IV. SUMMARY

In this work we present a combined study of the isospin-violating decay  $D_s^* \rightarrow D_s \pi^0$  and radiative decay  $D_s^* \rightarrow D_s \gamma$ . The isospin-violating decay  $D_s^* \rightarrow D_s \pi^0$  is investigated with both the tree-level  $\eta - \pi^0$  mixing and higher-order meson loop corrections from the intermediate  $D^{(*)}$  and  $K^{(*)}$  rescatterings. The radiative decay  $\Gamma(D_s^{*+} \rightarrow D_s^+ \gamma)$  is investigated in the same framework via the VMD model. Our findings indicate that the tree-level contributions are dominant in both processes, while loop effects play a crucial role in the understanding of the  $D_s^* \rightarrow D_s \pi^0$  decay. In particular, the  $D^* K^*$  rescatterings by exchange a  $K$  account for most of the loop corrections. In contrast, the loop corrections in  $\Gamma(D_s^{*+} \rightarrow D_s^+ \gamma)$  are negligibly small. With the experimental data for the branching ratio fraction, we obtain a better constraint on the coupling  $g_{J/\psi D \bar{D}}$ , which is crucial for a reliable estimate of the radiative decay width. These mechanisms can also help us understand other isospin-violating decay processes. Since the decay  $D_s^* \rightarrow D_s \pi^0$  is near the threshold of  $D_s^*$ , understanding this decay channel will aid in comprehending other near-threshold dynamics. Future precise measurement of the total width of  $D_s^*$  at BESIII is strongly recommended.

## ACKNOWLEDGEMENT

Useful discussion with Prof. Shi-Lin Zhu is acknowledged. This work is supported, in part, by the National Natural Science Foundation of China (Grant No. 12235018), DFG and NSFC funds to the Sino-German CRC 110 ‘‘Symmetries and the Emergence of Structure in QCD’’ (NSFC Grant No. 12070131001, DFG Project-ID 196253076), National Key Basic Research Program of China under Contract No. 2020YFA0406300, and Strategic Priority Research Program of Chinese Academy of Sciences (Grant No. XDB34030302).

- 
- [1] Medina Ablikim et al. Determination of spin and parity of  $D_s^*$  mesons. *Phys. Lett. B*, 846:138245, 2023.
- [2] T. M. Aliev, E. Iltan, and N. K. Pak. Radiative  $D^*$  Meson Decays in QCD Sum Rules. *Physics Letters B*, 334:169–174, 1994.
- [3] Hai-Yang Cheng, Chi-Yee Cheung, Guey-Lin Lin, Y. C. Lin, Tung-Mow Yan, and Hoi-Lai Yu. Corrections to Chiral Dynamics of Heavy Hadrons:  $SU(3)$  Symmetry Breaking. *Physical Review D: Particles and Fields*, 49(CLNS-93-1189, IP-ASTP-01-93, ITP-SB-93-03):5857–5881, 1994.
- [4] Ho-Meoyng Choi. Light-Front Quark Model Analysis of Heavy Meson Radiative Decays. *Journal of The Korean Physical Society*, 53:1205, 2008.
- [5] Hong-Bo Deng, Xiao-Lin Chen, and Wei-Zhen Deng. Meson Decays in an Extended Nambu–Jona-Lasinio Model with Heavy Quark Flavors. *Chinese Physics C*, 38(1):013103, 2014.
- [6] G. C. Donald, C. T. H. Davies, J. Koponen, and G. P. Lepage. Prediction of the  $D_s^*$  Width from a Calculation of Its Radiative Decay in Full Lattice QCD. *Physical Review Letters*, 112:212002, 2014.
- [7] Fayyazuddin and O. H. Mobarek. E1 and M1 Transitions in Quarkonia. *Physical Review D: Particles and Fields*, 48:1220–1224, 1993.
- [8] J. L. Goity and W. Roberts. Radiative Transitions in Heavy Mesons in a Relativistic Quark Model. *Physical Review D: Particles and Fields*, 64(JLAB-THY-00-45):094007, 2001.
- [9] A. N. Kamal and Q. P. Xu. Total Width of the  $D^*$ . *Physics Letters B*, 284(ALBERTA-THY-5-92):421–426, 1992.
- [10] Bo Wang, Bin Yang, Lu Meng, and Shi-Lin Zhu. Radiative Transitions and Magnetic Moments of the Charmed and Bottom Vector Mesons in Chiral Perturbation Theory. *Physical Review D: Particles and Fields*, 100(1):016019, 2019.
- [11] Guo-Liang Yu, Zhen-Yu Li, and Zhi-Gang Wang. Analysis of the Strong Coupling Constant  $G_{D_s^* D_s \phi}$  and the Decay Width of  $D_s^* \rightarrow D_s \gamma$  with QCD Sum Rules. *The European Physical Journal C: Particles and Fields*, 75(6):243, 2015.
- [12] C. T. Tran, M. A. Ivanov, P. Santorelli, and Q. C. Vo. Radiative Decays  $D_s^* \rightarrow D_s \gamma$  in Covariant Confined Quark Model. *Chinese Physics C*, 48(2):023103, February 2024.
- [13] Chi-Yee Cheung and Chien-Wen Hwang. Three Symmetry Breakings in Strong and Radiative Decays of Strange Heavy Mesons. *The European Physical Journal C: Particles and Fields*, 76(1):19, 2016.
- [14] Peter L. Cho and Mark B. Wise. Comment on  $D_s^* \rightarrow D_s \pi^0$  decay. *Phys. Rev. D*, 49:6228–6231, 1994.
- [15] A. N. Ivanov. On the  $D_s^{*+} \rightarrow D_s^+ + \pi_0$  decay in the effective quark model with chiral  $U(3) \times U(3)$  symmetry. 5 1998.
- [16] Kunihiro Terasaki. Decays of Charmed Vector Mesons -  $\eta\pi^0$  mixing as an origin of isospin non-conservation -. 11 2015.
- [17] Bin Yang, Bo Wang, Lu Meng, and Shi-Lin Zhu. Isospin violating decay  $D_s^* \rightarrow D_s \pi^0$  in chiral perturbation theory. *Phys. Rev. D*, 101(5):054019, 2020.
- [18] Gustavo Burdman and John F. Donoghue. Union of chiral and heavy quark symmetries. *Phys. Lett. B*, 280:287–291, 1992.
- [19] Mark B. Wise. Chiral perturbation theory for hadrons containing a heavy quark. *Phys. Rev. D*, 45(7):R2188, 1992.
- [20] R. Casalbuoni, A. Deandrea, N. Di Bartolomeo, Raoul Gatto, F. Feruglio, and G. Nardulli. Phenomenology of heavy meson chiral Lagrangians. *Phys. Rept.*, 281:145–238, 1997.
- [21] Gang Li, Qiang Zhao, and Bing-Song Zou. Isospin violation in  $\phi$ ,  $J/\psi$ ,  $\psi$ ,  $\psi'$   $\rightarrow \omega \pi^0$  via hadronic loops. *Phys. Rev. D*, 77:014010, 2008.
- [22] Gang Li, Yuan-Jiang Zhang, and Qiang Zhao. Study of isospin violating  $\phi$  excitation in  $e^+e^- \rightarrow \omega \pi^0$ . *J. Phys. G*, 36:085008, 2009.
- [23] Qian Wang, Xiao-Hai Liu, and Qiang Zhao. Open charm effects in  $e^+e^- \rightarrow J/\psi \eta$ ,  $J/\psi \pi^0$  and  $\phi \eta_c$ . *Phys. Rev. D*, 84:014007, 2011.
- [24] Feng-Kun Guo, Christoph Hanhart, Gang Li, Ulf-G. Meissner, and Qiang Zhao. Effect of charmed meson loops on charmonium transitions. *Phys. Rev. D*, 83:034013, 2011.
- [25] Xiao-Hai Liu and Qiang Zhao. The Evasion of helicity selection rule in  $\chi(c1) \rightarrow VV$  and  $\chi(c2) \rightarrow VP$  via intermediate charmed meson loops. *Phys. Rev. D*, 81:014017, 2010.
- [26] Xiao-Hai Liu and Qiang Zhao. Further study of the helicity selection rule evading mechanism in  $\eta_c$ ,  $\chi_{c0}$  and  $h_c$  decaying to baryon anti-baryon pairs. *J. Phys. G*, 38:035007, 2011.
- [27] Yuan-Jiang Zhang, Gang Li, and Qiang Zhao. Towards a Dynamical Understanding of the Non- $D\bar{D}$  Decay of  $\psi(3770)$ . *Phys. Rev. Lett.*, 102:172001, 2009.
- [28] S. Navas et al. Review of Particle Physics. *Phys. Rev. D*, 110(3):030001, 2024.
- [29] Hai-Yang Cheng, Chun-Khiang Chua, and Amarjit Soni. Final state interactions in hadronic  $B$  decays. *Phys. Rev. D*, 71:014030, 2005.

- [30] Qian Wang, Gang Li, and Qiang Zhao. Open charm effects in the explanation of the long-standing ‘ $\rho\pi$  puzzle’. *Phys. Rev. D*, 85:074015, 2012.
- [31] Ye Cao and Qiang Zhao. Study of weak radiative decays of  $D_0 \rightarrow V\gamma$ . *Phys. Rev. D*, 109(9):093005, 2024.
- [32] J. Gasser and H. Leutwyler. Chiral Perturbation Theory: Expansions in the Mass of the Strange Quark. *Nucl. Phys. B*, 250:465–516, 1985.
- [33] Xiang Liu, Xiao-Qiang Zeng, and Xue-Qian Li. Study on contributions of hadronic loops to decays of  $J/\psi \rightarrow$ vector + pseudoscalar mesons. *Phys. Rev. D*, 74:074003, 2006.
- [34] Claudia Isola, Massimo Ladisa, Giuseppe Nardulli, and Pietro Santorelli. Charming penguins in  $B \rightarrow K^*\pi, K(\rho, \omega, \varphi)$  decays. *Phys. Rev. D*, 68:114001, 2003.
- [35] Ye Cao, Yin Cheng, and Qiang Zhao. Resolving the polarization puzzles in  $D_0 \rightarrow VV$ . *Phys. Rev. D*, 109(7):073002, 2024.
- [36] Gang Li and Qiang Zhao. Hadronic loop contributions to  $J/\psi$  and  $\psi'$  radiative decays into  $\gamma\eta_c$  or  $\gamma\eta'_c$ . *Physics Letters B*, 670(1):55–60, December 2008.
- [37] Zi-wei Lin and C. M. Ko. A Model for  $J/\psi$  absorption in hadronic matter. *Physical Review C: Nuclear Physics*, 62:034903, 2000.
- [38] Ricardo D’Elia Matheus, F. S. Navarra, M. Nielsen, and R. Rodrigues da Silva. The  $J/\psi DD$  vertex in QCD sum rules. *Physics Letters B*, 541:265–272, 2002.
- [39] Yong-seok Oh, Taesoo Song, and Su Hounng Lee.  $J/\psi$  absorption by  $\pi$  and  $\rho$  mesons in meson exchange model with anomalous parity interactions. *Physical Review C: Nuclear Physics*, 63:034901, 2001.
- [40] Yongseok Oh, Wei Liu, and C. M. Ko.  $J/\psi$  absorption by nucleons in the meson-exchange model. *Physical Review C: Nuclear Physics*, 75:064903, 2007.
- [41] M. Ablikim et al. Measurement of branching fraction of  $D_s^{*+} \rightarrow D_s^+ \pi^0$  relative to  $D_s^{*+} \rightarrow D_s^+ \gamma$ . *Phys. Rev. D*, 107(3):032011, 2023.